

UC Berkeley

Climate Change

Title

Scenarios to Evaluate Long-Term Wildfire Risk in California: New Methods for Considering Links Between Changing Demography, Land Use, and Climate

Permalink

<https://escholarship.org/uc/item/53c1n0c2>

Authors

Bryant, Benjamin P.
Westerling, Anthony L.

Publication Date

2012-07-01

**Public Interest Energy Research (PIER) Program
White Paper**

**SCENARIOS TO EVALUATE LONG-
TERM WILDFIRE RISK IN
CALIFORNIA:**

**New Methods for Considering Links
Between Changing Demography,
Land Use, and Climate**

A White Paper from the California Energy Commission's California Climate Change Center

Prepared for: California Energy Commission

Prepared by: Pardee RAND Graduate School
University of California, Merced

JULY 2012

CEC-500-2012-030

Benjamin P. Bryant
Pardee RAND Graduate School

Anthony L. Westerling
University of California, Merced



DISCLAIMER

This paper was prepared as the result of work sponsored by the California Energy Commission. It does not necessarily represent the views of the Energy Commission, its employees or the State of California. The Energy Commission, the State of California, its employees, contractors and subcontractors make no warrant, express or implied, and assume no legal liability for the information in this paper; nor does any party represent that the uses of this information will not infringe upon privately owned rights. This paper has not been approved or disapproved by the California Energy Commission nor has the California Energy Commission passed upon the accuracy or adequacy of the information in this paper.

ACKNOWLEDGEMENTS

The authors would like to thank Jacquelyn Bjorkman and Jim Thorne for extensive discussion and support in our use of the UPlan scenarios. Alexandra Syphard also provided helpful insights and summary data that helped inform our parameter choices. We are grateful to three anonymous reviewers who provided constructive comments that greatly enhanced readability and clarity of the paper.

PREFACE

The California Energy Commission's Public Interest Energy Research (PIER) Program supports public interest energy research and development that will help improve the quality of life in California by bringing environmentally safe, affordable, and reliable energy services and products to the marketplace.

The PIER Program conducts public interest research, development, and demonstration (RD&D) projects to benefit California. The PIER Program strives to conduct the most promising public interest energy research by partnering with RD&D entities, including individuals, businesses, utilities, and public or private research institutions.

PIER funding efforts are focused on the following RD&D program areas:

- Buildings End-Use Energy Efficiency
- Energy Innovations Small Grants
- Energy-Related Environmental Research
- Energy Systems Integration
- Environmentally Preferred Advanced Generation
- Industrial/Agricultural/Water End-Use Energy Efficiency
- Renewable Energy Technologies
- Transportation

In 2003, the California Energy Commission's PIER Program established the California Climate Change Center to document climate change research relevant to the states. This center is a virtual organization with core research activities at Scripps Institution of Oceanography and the University of California, Berkeley, complemented by efforts at other research institutions.

For more information on the PIER Program, please visit the Energy Commission's website <http://www.energy.ca.gov/research/index.html> or contact the Energy Commission at (916) 327-1551.

ABSTRACT

This paper describes the development and analysis of over 21,000 scenarios for future residential wildfire risk in California on a 1/8-degree latitude/longitude grid at a monthly time step, using statistical models of wildfire activity and parameterizations of uncertainties related to residential property losses from wildfire. This research explored interactions between medium-high and low emissions scenarios, three global climate models, six spatially explicit population growth scenarios derived from two growth models, and a range of values for multiple parameters that define vulnerability of properties at risk of loss due to wildfire. These are evaluated over two future time periods relative to a historic baseline. The study also explored the effects of the spatial resolution used for calculating household exposure to wildfire on changes in estimated future property losses. The goal was not to produce one single set of authoritative future risk scenarios, but rather to understand what parameters are important for robustly characterizing effects of climate and growth trajectories on future residential property risks in California. Overall, by end of century, results showed that variation across development scenarios accounts for far more variability in statewide residential wildfire risks than does variation across climate scenarios. However, the most extreme increases in residential fire risks result from the combination of high-growth/high-sprawl scenarios with the most extreme climate scenarios considered here. Furthermore, this study shows that the sign of overall statewide risk in the highest growth cases depends on key parameters describing how expected losses vary with increasing housing value at the local level. The paper features case studies for the Bay Area and the Sierra foothills to demonstrate that, while land use decisions can have a profound effect on future residential wildfire risks, the effects of diverse growth and land use strategies vary greatly around the state.

Keywords: Fire, wildfire, risk, climate, scenario, WUI, wildland-urban interface, spatial

Please use the following citation for this paper:

Bryant, B. P., and A. L. Westerling. 2012. *Scenarios to Evaluate Long-Term Wildfire Risk in California: New Methods for Considering Links Between Changing Demography, Land Use, and Climate*. California Energy Commission. Publication number: CEC-500-2012-030.

TABLE OF CONTENTS

Acknowledgements	i
PREFACE	ii
ABSTRACT	iii
TABLE OF CONTENTS	iv
Section 1: Introduction	1
1.1 Climate Change and Residential Wildfire Risk	1
1.2 Ecological Context of Human Interactions with Fire.....	2
Section 2: Conceptual Model of Long-Range Wildfire Risk and Available Scenario Data	4
2.1 Conceptual Linkages Between Growth, Fire, and Risk	4
2.2 Summary of Non-growth Scenario Data Used in the Fire Probability Model	6
2.2.1 Historical Climatic, Hydrologic, and Land Surface Characteristics Data.....	6
2.2.2 Projected Climate and Hydrologic Data.....	7
2.2.3 Fire History Data.....	7
2.3 Spatially Explicit Population Growth Scenarios.....	8
2.3.1 Integrated Climate and Land Use Scenarios	9
2.3.2 UPlan Growth Scenarios for California	9
Section 3: Formalizing and Implementing the Residential Wildfire Risk Model	11
3.1 A Nested Model of Residential Wildfire Risk.....	11
3.2 Fire Probability Model.....	12
3.3 Conditional Probability of Tract Falling Within a Fire Perimeter.....	14
3.3.1 Baseline Probability of Vegetated Area Burning	15
3.3.2 Value-Based Probability Scaling	16
3.3.3 Scenarios to Vary Exposure Within Grid Cells.....	19
3.4 Loss Conditional on Tract in Fire Perimeter	21
3.5 Calculation of Aggregate Relative Risk	22
3.6 Growth Patterns as Multi-faceted Driver of Fire Probabilities and Exposure	22
3.7 Integrating UPlan and ICLUS Data Sets for Scenario Runs.....	25

3.8 Design of Computational Experiments.....	26
Section 4: Results	28
4.1 Statewide Wildfire Area Burned under Varying Climate and Growth Scenarios.....	28
4.2 Statewide Changes in Expected Losses under Varying Climate and Growth Scenarios.....	29
4.3 Sources of Variation: Climate, Growth, and Land Use.....	30
4.3.1 Climate and Growth Impacts	30
4.3.2 Impact of Land Use Decisions.....	34
4.4 Impact of Fire Risk Parameters	35
4.5 Discussion of Uncertainties and Caveats.....	37
Section 5: Conclusion	39
References.....	42
Glossary	47
APPENDIX A.1 Identifying New Populations for UPlan	48
Appendix A.2 Identifying Vegetated Areas Based on New Growth	49
Appendix A.3: County Map for California	51

LIST OF TABLES

Table 1: Types of Wildfire Impacts.....	2
Table 2: ICLUS Scenarios Factorial Study Design	26
Table 3: UPlan Scenarios Factorial Study Design.....	27
Table 4. Pairwise Performance of UPlan Scenarios for the San Francisco Bay Area and the Sierra Nevada Foothills	35
Table A1: Raster Mappings for UPlan Housing Densities	48

LIST OF FIGURES

Figure 1: Conceptual Model of How Climate Change and Growth Affect Long-Term Fire Risk..	6
Figure 2: Different plausible relationships for how tract density influences the likelihood of a tract falling within a fire perimeter, as captured by the scaling function $s(V, D, k, \alpha)$. The x-	

intercept is defined by D (located at the two vertical red lines in this plot), while curvature is described by the shape parameter k 18

Figure 3: The implementation and detailed dependencies of the conceptual model in Figure 2. With the exception of initial UPlan and ICLUS data, all data sources and final outputs are at the level of the 1/8 degree grid cell, with the final product aggregated to the state level for most of our results. Grey boxes indicate external data products used as inputs, rounded boxes are functions or algorithms, rectangles are data products we produced, and rectangles with diagonal corners indicate parameters or scenario input we developed. 24

Figure 4: Statewide Wildfire Burned Area Scenarios for 2035–2064 and 2070–2099 Expressed as a Ratio to the Average Modeled for 1961–1990 (with Year 2000 Population and Land Use). Each UPlan boxplot summarizes 729 scenarios, while each ICLUS boxplot summarizes 162 scenarios. Constant (CNST) scenarios hold population and footprint constant at year 2000 levels; each CNST boxplot summarizes 54 scenarios..... 28

Figure 5: Statewide Relative Risk by Period, Broken Out by Growth Scenarios, Assumed WUI/Urban Thresholds, and Climate. Dashed red line represents no change in risk. 29

Figure 6: Spatial Variation in Wildfire Risk for the San Francisco Bay Area Using the Ratio of ICLUS 2070–2099 Scenarios to Risk Estimated for the Base Period. Six scenarios illustrate the effects of climate change, growth scenario, and WUI exposure on residential property risk. A relative risk of 1 is equal to no change; therefore, green cells represent reductions in risk. White cells are not modeled. Other parameters are fixed across all six scenarios: WUI/Urban threshold: 1000 HH/km², Vegetation allocation method (VEG): Neutral, Scaling function concavity parameter (k): 0.333, Protection normalization: yes, Resolution: 100 m. 32

Figure 7: Spatial Variation in Wildfire Risk for the Sierra foothills Using the Ratio of ICLUS 2070–2099 Growth Scenarios to Risk Estimated for the Base Period: Six scenarios illustrate the effects of climate change, growth scenario, and WUI exposure on residential property risk. A relative risk of 1 is equal to no change; therefore, green cells represent reductions in risk. White cells are not modeled. Other parameters are fixed across all six scenarios: WUI/Urban threshold: 1000 HH/km², Vegetation allocation method (VEG): Neutral, Scaling function concavity parameter (k): 0.333, Protection normalization: yes, Resolution: 100 m. 33

Figure 8: Relative Marginal Effect of High-Growth Compared to Low-Growth Scenario in 2070–2099, Grouped by Different Scaling Function Parameters. The interaction of the two has a strong influence on whether future growth increases or decreases expected losses statewide..... 36

Figure A.3.1: County map for California with county names labeled for subregions discussed in Section 4..... 51

Unless otherwise noted, all tables and figure are provided by the author.

Section 1: Introduction

1.1 Climate Change and Residential Wildfire Risk

Wildfires in California routinely threaten people and property, destroy homes, force evacuations, expose large populations to unhealthful air, and result in the death or injury of some citizens and firefighters. Climate change may affect the size and frequency of wildfires in California, and its impacts are likely to vary substantially across the state (Westerling et al. 2011a; Bowman et al. 2009; Krawchuk et al. 2009; Westerling and Bryant 2008; Westerling et al. 2006; and Lenihan et al. 2003). And while wildfire poses many hazards, its most direct impacts on humans are fundamentally connected to how people are distributed over the landscape. In previous work (Bryant and Westerling 2009), we considered how changes in the probability of large fire events interact with changes in land use to affect residential property risks, drawing on a small number of scenarios for future climate, land use, and growth. In this paper, we expand the number of climate, land use, and growth scenarios considered, and also consider additional uncertainties and a more sophisticated model of expected housing loss due to wildfire, to more robustly characterize future changes in wildfire and wildfire-related residential property risk in California. A complementary study (Hurteau et al. in preparation) applies our results to assess changes in wildfire emissions of greenhouse gases and air pollutants.

This paper's primary aim is to describe how climate change and human development patterns over California may interact to lead to differing levels of fire-caused risk to residential property, with a greater focus on the relative impacts of different climate, population growth, and land use scenarios, as well as parameters related to fire management. This study used climate scenarios derived from three global climate models (GCMs) from the Intergovernmental Panel on Climate Change (IPCC)'s Fourth Assessment forced with medium-high and low emissions pathways (IPCC 2000, 2007). Our growth scenarios are derived from two different sets of spatially explicit raster data sets, each describing different twenty-first century population growth and land use scenarios. One set is based on work by Theobald (2005) and developed by the U.S. Environmental Protection Agency (U.S. EPA 2008) as the Integrated Climate and Land Use Scenarios (ICLUS) for the United States, and is provided at 100 meter (m) resolution. The other set is provided at 50 m resolution and generated using the UPlan growth model, developed for California by Thorne et al. (2012). As in Bryant and Westerling (2009), the primary results of this study are in the form of statistics on aggregate statewide relative risk, where the reference period is defined based on year 2000 development patterns and late twentieth-century (1961–1990) simulated climate. This paper also presents spatial distributions of changes in wildfire probabilities and expected losses to illustrate how these impacts can vary throughout the state.

In the remainder of the paper, we first review some impacts of wildfires. In Section 2, we develop our conceptual model and describe the data we have available for implementing such a model. In Section 3, we build up a formal model for estimating changes in wildfire risk; in the process clarifying our assumptions and how we handle the significant uncertainties inherent in

considering long-term scenarios of such risk.¹ Section 4 discusses the study’s primary findings, including changes in aggregate statewide risk and also some sub-regional analysis, while Section 5 summarizes the results and considers their policy implications.

1.2 Ecological Context of Human Interactions with Fire

While this work focuses on risks to residential property, there are many other less-obvious impacts, both to humans and also to ecosystems, some of which are listed in Table 1. (See the California Board of Forestry’s California Fire Plan [1996] for an extremely thorough attempt at comprehensively assessing wildfire impacts of all sorts). This paper focuses only on quantifying changes in direct damages to homes; therefore, when evaluating this study’s results, it is important to remember that these impacts represent just a fraction of the total impacts from wildfire. While monetization of many of the impacts listed in Table 1 is difficult and fraught with uncertainty, the California Department of Forestry estimated that, for example, watershed impacts of wildfire, in the form of soil erosion and potential required sediment removal from water bodies, may easily average out to magnitudes on the order \$100 per acre burned, possibly even up to thousands of dollars per acres burned in some cases (California Forestry Board 1996). This translates to at least tens of millions of dollars of annual impacts from that source alone. In addition, many of the environmental impacts have human consequences. The health and viewshed impacts of reduced air quality are readily apparent, but there are other more subtle and second-order effects, such as watershed impacts reducing desired fish populations and reducing power generation ability from hydroelectric dams.

Table 1: Types of Wildfire Impacts

Direct Human Impacts	Indirect Impacts
Structures burned/property value lost	Watersheds-soil loss, deposits
Prevention and suppression expenditures	Timber loss
Evacuation costs/lost productivity	Habitat disruption
Lives lost and adverse health effects of smoke	Species loss
Diminished recreational opportunities and viewsheds	Non-native species invasion
Disruption to infrastructure availability	

¹ In the interest of providing a relatively self-contained document, this paper incorporates a small amount of text from a previous white paper by the same authors, also written for the California Energy Commission (CEC-500-2009-048-F). These sections are primarily related to background material, while methods have since been enhanced and all of the results are based on new modeling work.

When considering damages, it is important to acknowledge that wildfire is in principle a natural phenomenon that serves a role in maintaining healthy ecosystems, but human presence and action combine to make fire both a risk to humans, and also potentially a risk to ecosystems. This is due to humans causing unnatural *patterns* of wildfire with intensities or frequencies outside the range of natural variability (Dellasala et al. 2004). For example, Stephens et al. (2007) estimate that fire suppression and land use changes reduced annual burned area in California forests from pre-settlement levels by more than 90 percent in the twentieth century. This long-term exclusion of wildfire may have led to increases in biomass and changes in fuel structure in some California forests that in turn have fostered hotter, more-intense forest wildfires that are harder to manage and may have had undesirable effects in forest ecosystems that are not adapted to high-severity fire (Gruell 2001; Allen et al. 2002; Miller et al. 2009). For another example, wildfire in chaparral ecosystems may not have been significantly affected by fire suppression, but pressures from increased development and human ignitions may have increased wildfire frequency and fostered invasion by exotic species (Keeley and Fotheringham 2003; Syphard, Radeloff et al. 2007). These changes can affect ecosystems in undesirable ways that may or may not be proportional to the residential impacts addressed here. With the importance of these ecological considerations in mind, we now turn to our focus on the risk of housing destruction due to wildfires.

Section 2: Conceptual Model of Long-Range Wildfire Risk and Available Scenario Data

Climate change impacts wildfire characteristics, as does human development on the landscape (growth). In turn, changes in wildfire characteristics affect the risk posed to that same human development. This section outlines these interactions at a high level, and discusses historical and modeled data available to us for considering different futures in a more quantitative way. The following section then formalizes these considerations into a quantitative risk model, in which risk is framed as expected losses of residential housing units to wildfire.

2.1 Conceptual Linkages Between Growth, Fire, and Risk

On seasonal to interannual time scales, climate–fire relationships describe the response of existing ecosystems to climate variability that affects fuel availability and flammability, with the relative importance of each varying significantly with ecosystem characteristics (e.g., Girardin et al. 2009; Krawchuk and Moritz 2011; Littell et al. 2009; Westerling 2010; Westerling et al. 2003). Climatic effects that influence the availability of fine surface fuels (grasses, forbs) tend to dominate in dry, sparsely vegetated ecosystems, while effects on flammability tend to dominate in moister, more densely vegetated ecosystems, although there is often not a clear partition between the two effects (Krawchuk and Moritz 2011; Littell et al. 2009; Westerling 2010; Westerling et al. 2003). On decadal timescales, shifts in climate that affect the spatial ranges of vegetation assemblages, and/or their productivity, have the potential to qualitatively alter fire regime responses to shorter-term climate variability.

In this study, the statistical fire models used allow a focus on how fire in existing ecosystems may respond to climate change, while the ecosystems themselves and their fire–climate relationships are implicitly assumed to remain fixed (as in Westerling et al. 2011a). To the extent that projected changes in climate and the resulting disturbance regimes may lead to qualitative changes in ecosystem responses to climate variability, these models may exhibit potentially significant biases, particularly for the warmest, driest scenarios toward the end of the century.

As with climatic variables, vegetation, and their attendant fire patterns, the distribution of people over the landscape also changes with time, and impacts eventual expected losses due to fires (fire risk). In fact, all of these changes are potentially linked to each other, though some links are stronger than others. Furthermore, changes in one variable may increase risk through one link while decreasing it through another. As an example of this phenomenon, development in a given region decreases the vegetation footprint available for the ignition of wildfires, but human presence may more than compensate by an increase in human-caused ignitions. However, the increased presence of humans may sometimes decrease fire size in the region, through early identification of fires and increased suppression efforts.² In general, the statistical

² The relationships between human presence, ignitions, and fire size are quite complex. The fire history data used here indicate that most large fires in coastal southern California are ignited by human activities; whereas, lightning ignitions play a more important role in Northern California forests. The

relationship between population density and the human-related “risk of fire” is some form of inverted U (or even one having multiple maxima), being zero at zero human presence, and zero at some saturated density (at an appropriately defined spatial scale), where everything is urban and wildfires cannot exist (Guyette et al. 2002). However, the range of shapes possible in between these extremes in our study area is not known, and likely highly contingent on many other variables associated with the locality.

To capture this dynamic and others, our model of fire risk accounts for human impacts on wildfire probabilities, and also allows for human development to act in ways that mitigate their exposure to fire proportionally with the value at risk, where *exposure* describes the expected losses entailed by the occurrence of a fire event. These relationships are shown conceptually below (Figure 1). Global growth scenarios affect emissions that drive climate change. Local growth scenarios, which are not necessarily coupled to global growth patterns, generate spatially explicit population trajectories through time. As modeled by Westerling et al. (2011a), this population distribution, together with climate change, affects wildfire occurrence and burned area, both directly and through their joint impact on vegetation change.

However, understanding changes in wildfire risk in terms of the potential loss of homes requires additional information beyond fire probabilities and burned areas: It requires an estimate of how those spatially explicit fire patterns interact with spatially explicit changes in housing across the state. Large increases in fire occurrence where there are no homes do not increase risk of housing loss, while new growth in a fire-prone area may dramatically increase risk even under unchanging fire behavior. Therefore, the focus of the present paper is on transforming scenarios of spatially explicit population growth into estimates of value exposed to loss from wildfire, and then linking those exposed value estimates to fire probabilities to generate estimates of overall risk.

We next present the data available to us for this task. Our treatment of the data specific to estimating fire probabilities is highly condensed, because there are many data sources (these are summarized graphically in Figure 3, which follows the detailed model description), and their use in generating fire probabilities and burned area has been described elsewhere, such as in Westerling et al. (2011a).

large populations in coastal southern California and other areas of the state adjacent or easily accessible to urban population centers may imply a saturation of potential ignition sources in many parts of the state in recent decades (see Guyette et al. 2002). At the same time, only large fires (>200 hectares, ha) are modeled here. The vast majority of wildfires reported in the state are below that threshold and excluded from analysis, while the vast majority of burned area is accounted for by the largest fires. Climate exerts a strong influence on whether ignitions—human or natural—can spread into fires larger than 200 ha. Consequently, the number of large fires may not be as sensitive to variability in human ignitions as it is to other factors, including climate. More difficult issues for predicting burned area accurately are clustering in lightning ignitions in northern California, such as in 1987 and 2008, and high wind events that fatten the extreme tail of the fire size distribution but do not significantly affect the number of ignitions.

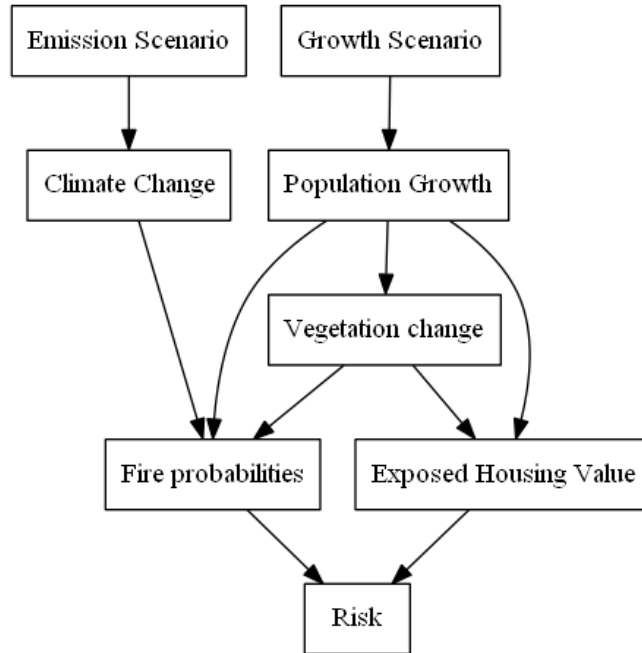


Figure 1: Conceptual Model of How Climate Change and Growth Affect Long-Term Fire Risk

2.2 Summary of Non-growth Scenario Data Used in the Fire Probability Model

2.2.1 Historical Climatic, Hydrologic, and Land Surface Characteristics Data

A common set of historical climate data, including gridded maximum and minimum temperature and precipitation and simulated hydrologic data, were assembled by the California Climate Change Center at the Scripps Institution of Oceanography for the 2006 California Scenarios project and the subsequent California Vulnerability and Adaptation project. Gridded daily climate data (temperature, precipitation) derived from historical (1950–1999) station observations were obtained online from Santa Clara University (see Maurer et al. 2002; Hamlet and Lettenmaier 2005; <http://www.engr.scu.edu/~emaurer/data.shtml>). Westerling et al. (2011a) then used these data with wind speed, topographic, and vegetation data to force the Variable Infiltration Capacity (VIC) macroscale hydrologic model at a daily time step in full energy mode with climatologic winds, producing hydroclimatic variables such as actual evapotranspiration, surface temperature, and snow water equivalent (Liang et al. 1994). The VIC model solves for water and energy balances given daily temperature, precipitation, and wind speed values as inputs. Westerling et al. (2011a) used the Penman-Monteith equation to estimate potential evapotranspiration (Penman 1948; Monteith 1965) and then calculated moisture deficit (potential minus actual evapotranspiration).

For the VIC inputs, Westerling et al. (2011a) used coarse vegetation categories based on the University of Maryland vegetation classification scheme with fractional vegetation adjustment (Hansen et al. 2000) and topographic data on a 1/8-degree grid obtained from the North

American Land Data Assimilation System (LDAS, see Mitchell et al. 2004; accessed online at <http://ldas.gsfc.nasa.gov/>). The LDAS topographic layers are derived from the GTOPO30 Global 30 Arc Second (~1kilometer [km]) Elevation Data Set (Mitchell et al. 2004; Gesch and Larson 1996; Verdin and Greenlee 1996). The LDAS data also provided inputs for the (Westerling et al. 2011a) fire models used in this study, including gridded aspect and vegetation fractions. Wind speed data for 1950–1999 were accessed online from the National Centers for Environmental Prediction (NCEP) Reanalysis project (<http://www.esrl.noaa.gov/psd/data/reanalysis/>) and used to calculate a monthly wind speed climatology interpolated to the LDAS grid for use in the VIC hydrologic simulations. Relative humidity and shortwave radiation values used in VIC were derived from the MT-CLIM algorithm, version 4.2, using temperature and precipitation as inputs (see Kimball et al. 1997; Thornton and Running 1999; Pierce and Westerling in review).

2.2.2 Projected Climate and Hydrologic Data

Cayan et al. (2009) obtained and downscaled twelve future climate scenarios for the California Vulnerability and Adaptation project, and used temperature and precipitation from these scenarios to force VIC hydrologic simulations, as described for the historical data above. A subset of six of those future climate scenarios are used here, derived from three global climate models (GCMs) (National Center for Atmospheric Research [NCAR] PCM 1, Centre National de Recherches Météorologiques [CNRM] CM 3.0, and Geophysical Fluid Dynamics Laboratory [GFDL] CM 2.1) from the Intergovernmental Panel on Climate Change's (IPCC) Fourth Assessment (AR4), forced with medium-high and low emissions pathways (the Special Report on Emissions Scenarios SRES A2 and SRES B1scenarios). These scenarios were downscaled by Cayan et al. (2009) using the bias-corrected constructed analogues method (Maurer et al. 2010.)

While the PCM 1 model from NCAR is an older-generation model that is not as up to date as the others, it was included because it is an outlier among the IPCC models, with lower climate sensitivity and smaller temperature increases over California than most other models. The CNRM and GFDL model sensitivities span the middle of the range of temperature projections available for California, but not the warmest scenarios that have been projected for the region. The NCAR model used here tends to have insignificant changes in precipitation over California by end of century, while the GFDL and CNRM models tend to project decreased precipitation (Cayan et al. 2009). Even where precipitation does not change significantly, increased temperatures can lead to drier fuels through increased evaporation and transpiration. Thus the scenarios used here span the lower to intermediate range projections for warmer, mostly drier conditions over California.

2.2.3 Fire History Data

While fire ignitions may be plentiful, most wildfires are too small to be consequential. Typically, a small fraction of all fires generates the vast majority of the total area burned, suppression costs, and damages (e.g., Strauss et al. 1989; Johnson 1992; Strategic Issues Panel on Fire Suppression Costs 2004). Documentary records of larger fires also tend to be more comprehensive and higher quality, probably because of their greater economic and ecological consequences, and focusing on the small subset of large fires results in data that are more

tractable to quality assurance efforts (Westerling et al. 2006). Therefore, we restrict our analysis to fires exceeding 200 hectares (ha) in size.³

Westerling et al. (2011a) used fire history (1980–1999) data to estimate the fire models employed here and described in Section 3.2. Their data are an extension and update of the data sets used in Westerling et al. (2006), with the data methodology described in the online supplementary materials to Westerling et al. (2006). The portion of their fire history used here incorporates documentary records from the California Department of Forestry and Fire Protection (CalFire), county fire departments under contract with CalFire, U.S. Department of Interior agencies (Bureau of Land Management, Bureau of Indian Affairs, National Park Service), and the U.S. Department of Agriculture (Forest Service) to produce a comprehensive record of large fires covering most of the state and federal protection responsibility areas in California.⁴ These are for wildfires that were classified as “action” or “suppression” fires, as opposed to prescribed or natural fires used to meet vegetation management goals. These data were aggregated by month on a 1/8-degree latitude and longitude grid, producing numbers of large fires and total area burned in those fires by the month and grid cell in which the fires were reported to have ignited. The fire probabilities simulated here reflect associations with historical climate and land surface characteristics detected in these historical fire data for California.

2.3 Spatially Explicit Population Growth Scenarios

We use two sources of spatially explicit housing scenarios as inputs to several variables in our model, and increase the richness of our explorations by considering variations derived from each source. In both cases, the primary data source provides fine-resolution raster data, where each raster cell holds an expected housing density and an expected population per housing unit. We then use these data sources as inputs into the following:

- Population for the fire probability model
- Vegetation fractions used in both the fire probability model and the exposure model
- Initial vulnerable values in the exposure model

Appendices A.1 and A.2 describe our algorithmic transformations of the data to extract the above model inputs from the raw scenario data. Here we simply describe the data sources as they relate to our scenario modeling.

³ The arbitrary 200 ha threshold was selected for historical reasons: The Canadian Large Fire History uses a 200 ha threshold (Stocks et al. 2002), so a consistent threshold was used to facilitate creation of a western North American fire history. This threshold allows the creation of a comprehensive data set that captures most of the burned area in the region, and meets statistical requirements for selecting a threshold value for estimating generalized Pareto distributions (Holmes et al. 2008).

⁴ Local responsibility areas (LRAs) were excluded. LRAs are mostly urban and agricultural areas that account for most of the population of the state, but very few of its large wildfires.

2.3.1 Integrated Climate and Land Use Scenarios

The Integrated Climate and Land Use Scenarios (ICLUS) were developed to create thematically consistent land-use scenarios at high resolution across the United States (U.S. EPA 2008). They link country-level population growth assumptions with the Spatially Explicit Regional Growth Model (SERGoM) developed by Theobald (2005) to generate housing density projections at the 100 meter (m) level through the end of the twenty-first century. The ICLUS scenarios used for this study provide three different growth trajectories, originally intended to correspond with the SRES scenarios: A2 referred to a higher growth scenario relative to a base case (with a higher population growth and higher population per housing unit), and B1 referred to a lower growth population scenario. Because there need not be a strict correlation between the growth path of California and the global population storyline driving global climate, we vary these scenarios independently, and henceforth refer to ICLUS B1, base-case, and A2 scenarios as “low” “mid” and “high” to avoid confusion with the climate-specific scenarios, which we still refer to by their SRES labels of B1 and A2.

These projections were provided on a 100 m raster (where each cell is a “tract” as described in Section 3.1, and in contrast with the much larger 1/8 degree “grid cell”). Because of the sensitivity of our model to the density of tracts, and in turn the sensitivity of the density to the scale at which density is defined,⁵ we also aggregate the ICLUS data to higher levels—to cells with 200 m, 400 m, and 800 m sides—and perform our loss calculations for each case.

2.3.2 UPlan Growth Scenarios for California

The UPlan scenarios were developed specifically for California by Thorne et al. (2012) and offer a set of projections for how new growth is distributed spatially throughout California in the year 2050, with the same amount of population growth in each scenario. They have numerous strengths relative to ICLUS, but also possess some key drawbacks specific to modeling fire risk. Like ICLUS, they offer three growth scenarios,⁶ though unlike ICLUS they are not explicitly or conceptually tied to the SRES scenarios. One scenario is a business-as-usual case (“bau”), another refers to smart growth (“smart”), and another is premised on reducing development in areas assigned moderate or higher fire hazard severity ratings by CalFire (“fire”). It should be noted, however, that the fire hazard severity ratings are rather distinct from the risk measures generated here in that they account for fuel characteristics directly and are generally provided at a far finer spatial scale. Different hazard zones vary down to a minimum of 20 acres in size for urban areas and 200 acres for wildland areas. By contrast, one grid cell in our model is on

⁵ As an example to illustrate the importance of spatial scale, consider an urban threshold of 10 households per hectare, and a 200 m × 200 m cell, which is subdivided into four 100 m × 100 m cells. If three of the 100 m-scale cells contain nine households and one cell contains 17, one arrives at very different outcomes dependent on the spatial scale: Using the 100 m spatial scale, three cells would be vulnerable and one would be considered urban; whereas, at the 200 m scale the average density would be 11, and therefore all 4 hectares would be considered urban.

⁶ The study used scenarios and related spatial data made available in mid-2011. Additional scenarios have since been developed, as described in Thorne et al. (2012).

the order of 30,000 acres. These discrepancies may contribute to some of the non-intuitive results that are seen when comparing UPlan scenarios later on.

The UPlan data has a finer spatial resolution (50 m) compared to ICLUS, but the drawback of a coarser-density resolution, allowing new growth to occur in only a small number of discrete density classes (such as one housing unit per acre, five housing units per acre, and so on). Unlike the version of ICLUS we rely on, UPlan also has the advantage of explicitly projecting the future footprint of commercial and industrial growth and also allotting all new growth based on attractors that include actual county zoning plans. Unfortunately, while UPlan may better represent the processes of future growth, the drawback is that it does not rely on any explicit representation of the base year housing distribution, beyond assuming an urban mask in which new growth does not occur. This creates challenges when attempting to make valid risk estimates relative to a base year, which is addressed in Section 3.7.

Section 3: Formalizing and Implementing the Residential Wildfire Risk Model

This section establishes an expected loss framework of wildfire risk that ties together fire probabilities and expected losses contingent on fire events. We first briefly describe the statistical model used to arrive at spatially explicit fire probabilities. We then focus in great detail on how the study addressed the challenges of modeling expected losses when the joint spatial distribution of housing development and vegetation landscape cannot be predicted with any meaningful certainty at the fine spatial scales of our growth data. We then discuss and illuminate the many cross-linkages between climate, growth, fire, and exposure to wildfire risk, and exactly how our model links many data sources and intermediate data products to produce our ultimate risk estimates. Lastly, discusses how we created the computational experimental design that specified our many thousands of scenarios.

3.1 A Nested Model of Residential Wildfire Risk

We focus first on the overall model of expected losses due to wildfire within a grid cell R , which is composed of tracts of equal area that together partition R .⁷ In this modeling effort, the region R is a 1/8 degree grid cell mentioned above, and each tract is a raster cell as provided by either ICLUS or UPlan scenarios. Each region R is therefore approximately a rectangle with sides of 10–14 kilometers, and each tract is a square with sides between 50 and 400 meters (depending on the data source and parameter settings). Each tract τ_i ($i \in 1..N_\tau$) contains some value V_i , where *value* may be defined as monetary value, or, with increasing coarseness, the number of housing units or structures. Our analysis assumes that value is described by number of housing units, since that is how our growth scenario data was provided. To avoid spurious reliance on the very fine-grained detail provided by the growth scenarios, the study does not assume exact knowledge of the spatial distribution of housing units within the each cell, but instead uses that detailed information to create frequency distributions of tract values for each grid cell.

Following prior work (Westerling et al. 2011a and 2011b; Preisler et al. 2011; Westerling and Bryant 2008; and Preisler and Westerling 2007), we model a grid cell R as having a time-varying probability $P(F)$ of large fire occurrence, assumed to be a function $f_p(POP, VEG, C)$ of the population within the region (POP), fraction of the region that is vegetated (VEG), and other variables C , such as hydroclimate and diverse land surface characteristics. (Each of these sets of variables includes time-varying elements, but for notational simplicity we do not include time subscripts.) Any specific fire is associated with a perimeter that encompasses some subset of the tracts within R . And while the spatially explicit distribution of fire events is difficult to estimate, each tract can be considered to have some baseline probability of being encompassed by fire,

⁷ The equal area assumption is not necessary to implement our approach, but essentially holds true for our raster-based growth scenario data and simplifies presentation and implementation of the method.

conditional on a fire event within the region.⁸ We denote this $P(\tau_i \in \tau_F|F)$, where τ_F denotes the set of tracts encompassed by a fire. Then, by breaking out conditional probabilities, we can express the total expected loss within R as:

$$E(LOSS) = f_P(POP, VEG, C) \times \sum_{i=1}^{N_\tau} [P(\tau_i \in \tau_F|F) \times (L(V_i)|\tau_i \in \tau_F)] \quad (1)$$

This says that the expected loss in R is the probability of a fire within R multiplied by the sum of expected losses in each tract, given that there is a fire in R . The expected loss in each tract is similarly decomposed into the probability of that tract falling within a fire perimeter and the expected loss $L(V_i)$ contingent on a tract falling within a fire perimeter. We refer to this approach as *nested* because it identifies expected losses within each region by considering expected losses within each tract, contingent on a fire event. While “grid cell level conditional expected losses” would perhaps be the most accurate term to describe this latter concept, we refer to the right half of Equation 1 as “exposure” or “exposed value.” It is slightly at odds with some other definitions of exposure, but consistent with the idea that exposed value is what will be lost in the event of the main hazard (wildfire in the region) coming to pass.

While theoretically consistent, we do not necessarily have historical or modeled data to support the identification of every element of the above equation. The next section discusses each component of the above equation and the strategies used to estimate changes in risk while accounting for the uncertainty and data limitations.

3.2 Fire Probability Model

This study used Westerling et al.’s (2011a) logistic regression models and data (summarized in Sections 2.2.1–2.2.3) to estimate monthly probabilities of fires in state and federal protection responsibility areas in California that exceed 200 ha and 8500 ha occurring in a region R . These probabilities are described as functions of climate, simulated hydrology, land surface characteristics, population, and growth footprint; and R is a cell on a 1/8 degree latitude/longitude grid (see also Preisler et al. 2004). Area burned in these fires is estimated using generalized Pareto distributions (GPDs) fit to fires between 200 ha to 8500 ha and to fires > 8500 ha, assuming that the fire size distributions are stationary over time and space. Monthly estimates produced are then averaged over time periods 1961–1990, 2035–2064, and 2070–2099 to produce expected annual fires and expected annual areas burned for each region within those periods.

⁸ While somewhat cumbersome, we generally use the terminology of a tract “falling within a fire perimeter” rather than the far shorter “burning.” This is in recognition of the fact that modern fire protection approaches mean that sometimes housing structures may be encompassed within a fire perimeter but not actually burn, due to the successful creation of defensible space and appropriate construction techniques, among other factors. Our terminology is therefore a conceptual distinction and also one that is formally represented in our model.

Formally, the probability of a fire greater than 200 ha occurring in region R for a given month, denoted $P(F)$, is estimated using a logistic regression model of the form:

$$\begin{aligned} \text{Logit}(P(F)) &= \log(P / (1 - P)) \\ &= \beta \times [1 + D30 + D01 + D02 + PCP + \\ &\quad G(D30, AET30) \times (1 + TMP + CD0) + \\ &\quad G(TMP) + G(RH) + G(POP) \times (1 + D30) + G(VEG) + FRA] \end{aligned} \quad (2)$$

where:

β is a vector of parameters estimated from the data,

$G(\bullet)$ are matrices describing semi-parametric smooth transformations of the data as described in Preisler and Westerling (2007),

$G(D30, AET30)$ is a thin-plate spline that estimates a spatial surface as a function of 30-year average cumulative Oct.–Sep. moisture deficit ($D30$) and actual evapotranspiration ($AET30$) (Preisler and Westerling 2007; Preisler et al. 2011; we relied on modules for fitting thin-plate splines within R provided by the Geophysical Statistical Project (<http://www.cgd.ucar.edu/stats/Software/Fields>) that serves as a proxy for coarse vegetation characteristics (Westerling et al. 2011a online supplement),

$D01$ and $D02$ are the 1- and 2-year leading cumulative Oct.–Sep. moisture deficit,

$CD0$ is the cumulative Oct.–current month moisture deficit,

PCP is the 2-month cumulative precipitation through the current month,

$G(TMP)$ is the second-order polynomial transformation of monthly average surface air temperature,

$G(RH)$ is the second-order polynomial transformation of $RH = \log((x+.002)/(1-x+.002))$,

where x is monthly average relative humidity,

$G(VEG)$ is a degree 3 basis spline transformation of $VEG = \log((x+.002)/(1-x+.002))$, where x is the vegetation fraction,

$G(POP)$ is the second-order polynomial transformation of total population,

and FRA is $\log((x+.002)/(1-x+.002))$ where x is federal protection responsibility area as a fraction of total area,

The expected area burned, given that a fire greater than 200 ha occurs, is:

$$E(A(F)) = E(A(F) \mid A(F) < 8500) + P(F \mid A(F) > 8500) * E(A(F) \mid A(F) > 8500)$$

where $E(A(F) \mid A(F) < 8500)$ is the expected area burned by fires in the range of 200 to 8,500 ha, conditional on a fire greater than 200 ha occurring in the grid cell. This area is estimated from a truncated GPD fit to historical fires observed in California. Similarly,

$E(A(F) \mid A(F) > 8500)$ is the expected area burned given that at least 8500 ha burned, and $P(F \mid A(F) > 8500)$ is derived from the logistic regression:

$$\text{Logit}(P(F) \mid A(F) > 8500) = \beta \times [1 + RH + Aspect + USFS]$$

where $Aspect$ is the north/south component of aspect computed as $\cos(\pi/2 + aspect * \pi/180)$

and $USFS$ is $\log((x+.002)/(1-x+.002))$ where x is U.S. Forest Service protection responsibility area as a fraction of total area.

Because the GPD models are assumed to be stationary, $E(A(F) | A(F) < 8500)$ and $E(A(F) | A(F) > 8500)$ are constants. Climate affects expected area burned through its effects on $P(F)$ and $P(F | A(F) > 8500)$, which then determine area burned linearly. Similarly, changes in population affect estimates of $P(F)$ directly, as well as indirectly through the effects of population growth and its spatial footprint on the vegetation fraction, VEG (see Appendix A.2).

As described in Westerling et al. (2011a), future fire probabilities are produced by feeding to the statistical models described above the temperature and precipitation values from downscaled GCM outputs, as well as variables derived from VIC hydrologic simulations forced by downscaled GCM outputs. The methodology used here projects fire-vegetation-climate interactions of present day ecosystems as they are currently managed onto simulated future climates.

3.3 Conditional Probability of Tract Falling Within a Fire Perimeter

Issues of scale and data availability present a significant challenge when it comes to estimating the probability of a given tract being encompassed by fire (the $P(\tau_i \in \tau_F | F)$ of Equation 1). In reality, this probability is influenced by many factors, such as the location of the tract with respect to vegetation in the region, the location of the tract with respect to boundaries that fire cannot cross, and also induced protective efforts due to value within the tract. While such factors can be somewhat precisely identified or estimated for near-term risk assessments, we cannot possibly know these relationships for multitudes of tracts decades into the future; therefore, we attempt to bound the impact of such uncertainty.

The basic strategy is to decompose the probability of a given tract falling within a fire perimeter into three components that we can better estimate, confidently bound, or identify as irrelevant. These are:

- $P_0(\tau_i \in \tau_F | \tau_i \in \tau_{VEG})$, the baseline probability a generic vegetated tract will fall within a wildfire perimeter under the assumption that there is nothing of high value to induce greater protection of that tract,
- $s(V_i)$, a scaling adjustment to the above probability, to account for value-induced protective efforts that reduce the probability that a given tract will burn, and
- $P(\tau_i \in \tau_{VEG})$, the probability that a given tract (with associated value V_i) is vegetated and therefore has a nonzero probability of being encompassed by a wildfire.

Note that we have dropped the conditionality on F for convenience, as all equations for the remainder of this section assume a fire event.

Using the above expressions, the probability of a tract burning can be decomposed as follows:

$$P(\tau_i \in \tau_F) = P_0(\tau_i \in \tau_F | \tau_i \in \tau_{VEG}) \times s(V_i) \times P(\tau_i \in \tau_{VEG}) \quad (3)$$

Note also that the above equation makes the assumption that non-vegetated tracts are not at risk for loss due to wildfire, i.e., $P_0(\tau_i \in \tau_F | \tau_i \notin \tau_{VEG}) = 0$. In reality, homes near the boundary of vegetated areas may be at risk due to firebrands, house-to-house spread, and ignition from direct heat (Cohen 2008). With access to highly reliable fine-scale predictions for both housing development and vegetation patterns, one could utilize such data to include structures lying within some distance of urban/vegetation boundaries as vulnerable. We unfortunately cannot rely on such data due to the long-term nature of our scenario investigation. Instead, we consider multiple definitions for defining vegetated and urban areas that attempt to bound the value in tracts truly at risk. These are discussed next.

3.3.1 Baseline Probability of Vegetated Area Burning

We assume that, prior to adjusting for the existence of valuable structures on a tract, there is a common baseline probability that a given vegetated tract will fall within a wildfire perimeter during a large fire event: $P_0(\tau_i \in \tau_F | \tau_i \in \tau_{VEG})$. That is, given a fire that starts in a hypothetical region covered with some vegetated tracts and some non-vegetated tracts, *all of which have no housing value*, what is the probability that any given vegetated tract will fall within the fire perimeter? Rather than attempt to estimate this probability, we make the assumption that it stays constant across time and scenarios, and that it therefore becomes irrelevant when considering relative risk across time periods and scenarios. This is one of two elements of our model that we do not explicitly bound or estimate, as it is both challenging to do, and also unnecessary in order to arrive at relative risk estimates.

However, we emphasize that this assumption is not as strong as it may appear. First, it only applies to the baseline probability assuming all else is equal, and is adjusted later based on exposure at the tract level (discussed in Section 3.3.2)—thus it is not the case that we assume all tracts have equal likelihood of falling within a fire perimeter.⁹ Second, expected housing losses are driven by the structures in the tract, rather than simply by the number of tracts burned (though area burned is more strongly associated with other impacts of interest, and is given more focus in Westerling et al. 2011a). The variations in our scenarios for mapping exposed structures (in Section 3.3.3) should far outweigh any error or bias introduced by assuming constant baseline probabilities.

We did investigate a possible avenue for relaxing the assumption that $P_0(\tau_i \in F | \tau_i \in \tau_{VEG})$ stays constant over time and scenarios, which is to assume as a limiting case that the probability of a vegetated tract burning in a fire event is directly proportional to the expected size of a fire relative to the vegetated area. Mathematically, this would assume that:

$$P_0(\tau_i \in \tau_F | \tau_i \in \tau_{VEG}) = \min\left(\frac{E(A(F))}{A(\tau_{VEG})}, 1\right), \quad (4)$$

⁹ Formally, this assumption may be considered equivalent to the assumption of a uniform prior distribution in the Bayesian sense.

where $A(\cdot)$ denotes area of the fire or vegetated area. While perhaps valid for small perturbations around large vegetated areas, this method drastically exaggerates the impact of reducing vegetated area in future periods, and does so in a way that is discordant with the theory behind how the fire probability model is estimated.

3.3.2 Value-Based Probability Scaling

We assume that, all else equal, the more housing units there are within a tract of given area, the less likely it is to succumb to wildfire. This is partly due to the physical characteristics of fire spread, but also due to the induced protection: Firefighters and managers of wildfire risk may be more likely to direct effort to protecting clusters of many homes; whereas, fewer resources may be directed to protecting a lone, difficult-to-access cabin amid many acres of trees. In the limit, large, densely developed areas of land are physically incapable of supporting wildfires and are deemed urban. Together, these dynamics suggest that, at some sufficient level of statistical averaging, the probability that a tract falls within a fire perimeter ($P(\tau_i \in \tau_F)$) should be reasonably modeled as decreasing monotonically as V_i increases, until the tract reaches some threshold density value (which we label the wildland-urban interface [WUI]/urban threshold), beyond which it is equal to zero. We also treat the WUI/urban threshold as the threshold beyond which a tract cannot be considered vegetated.¹⁰ (Vegetation allocation is discussed in Section 3.6).

To capture the dynamics described above, we further adjust the probability of a tract being within a fire perimeter by a scaling function $s(V_i, D, k, \alpha)$, where D , k , and α are parameters. (We sometimes omit the parameters for convenient when referencing $s(V_i)$). Here D is the WUI/urban density threshold introduced above, α is the area or resolution over which value is considered when evaluating density, and k is a dimensionless shape parameter that controls the concavity of the function as V_i/α varies between 0 and D . While many functions could potentially capture the qualitative relationship, we use the following scaling function for s :

$$s(V_i, D, k, \alpha) = \begin{cases} \left[1 - \left(\frac{V_i/\alpha}{D} \right)^k \right]^{\frac{1}{k}} & \text{if } \frac{V_i}{\alpha} < D \\ 0 & \text{otherwise} \end{cases} \quad (5)$$

¹⁰ We recognize that these two concepts are not necessarily captured by the same exact density, and we also recognize that the assumption that a density alone can be used to define a threshold between urban WUI does not account for different WUI classifications such as intermix and interface. However, we believe that by exploring significant variation in both the density threshold *and the spatial scale at which density is evaluated*, we capture the range of impacts that a more detailed (and infeasible) treatment of the WUI might yield.

High values of k lead to overall greater exposure (as we define it), in that a rise in value within a tract does not significantly reduce the likelihood of that tract burning until that value nears the WUI/urban threshold, while low values of k (below one) imply that even a little value within the tract induces significant protection efforts.¹¹

Figure 2 illustrates some possible shapes captured in this framework. The location where the curves meet the X-axis is determined by D (with two different thresholds shown at the two vertical red lines), while their curvature is determined by k . Curves 1 ($D = 147$ households per square kilometer [HH/km²], $k = .333$) and 2 ($D = 147$ HH/km², $k = 3$) represent cases in which only relatively low-density tracts are considered vulnerable to wildfire, and 3 ($D = 1000$ HH/km², $k = 1$) and 4 ($D = 1000$ HH/km², $k = 3$) correspond to an assumption that tracts remain vulnerable up to a higher density (the densities shown are the values applied to the ICLUS data set). All else equal, an assumption that Curve 1 best described how probability of tracts burning is reduced as density increases would lead to the lowest expected losses, while Curve 4 would lead to the highest expected losses, since it considers a wider range of densities as vulnerable to wildfire, and value within the vulnerable range is not appreciably scaled down until very close to the high-density threshold.

If we let $s(V_i, D, k, \alpha)$ range from zero to unity, then it can only decrease the likelihood of tracts burning. However, we do not have sufficient empirical knowledge to say whether a value-induced reduction in probability on a given tract lowers the probability of only that tract falling within the fire perimeter, or whether it lowers it in part by increasing the probability that other tracts will succumb to wildfire instead. One might imagine that in circumstances where fire-fighting resources are constrained, protecting certain tracts may leave other low-value tracts more vulnerable than they were otherwise, and so the total number of tracts encompassed by fire does not diminish significantly. Therefore we explore both possibilities by considering the full reduction case in which the output of $s(V_i, D, k, \alpha)$ ranges between zero and unity, but we also consider a case in which the total probability of tracts burning is fully conserved within the region R . In this case $s(V_i, D, k, \alpha)$ is used to identify initial weights on probabilities within $[0,1]$, which are then normalized to sum to the total number of vegetated tracts. Specifically, under the assumption of normalization, we scale by \hat{s} instead of s , as follows:

$$\hat{s}(V_i, D, k, \alpha) = \frac{N_{VEG} s(V_i, D, k, \alpha)}{\sum_{i \in \tau_{VEG}} s(V_i, D, k, \alpha)} \quad (6)$$

¹¹ For reasons of numerical convenience related to ensuring consistency between urban, vegetated, and vulnerable tracts, we consider scaling values for $V_i/\alpha \leq D$ to be bounded from below at a small positive value (10^{-6}), while values strictly above the threshold receive a scaling value of zero.

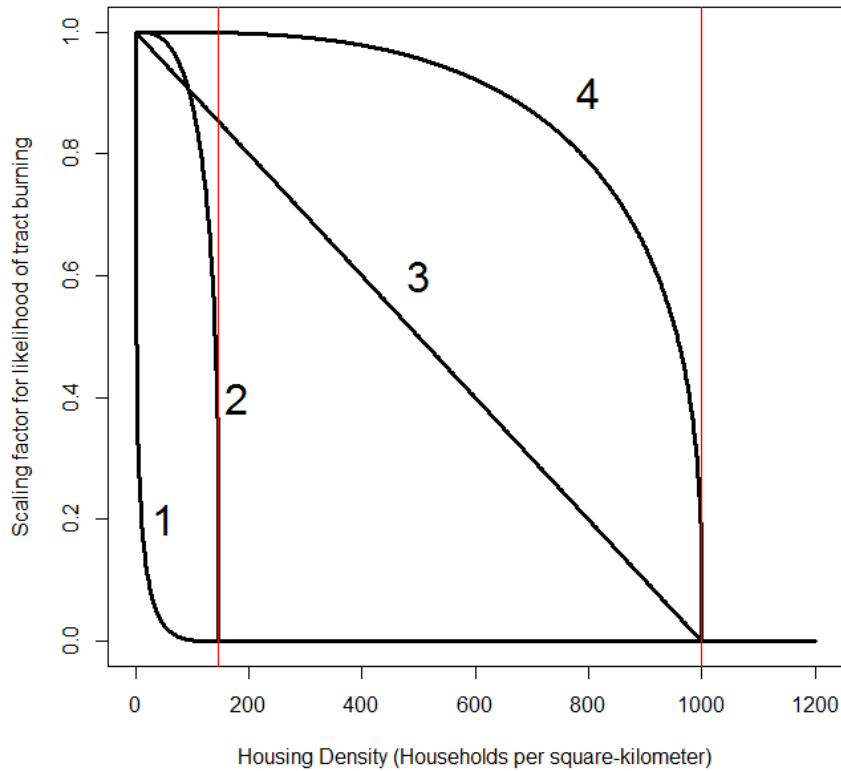


Figure 2: Different plausible relationships for how tract density influences the likelihood of a tract falling within a fire perimeter, as captured by the scaling function $s(V, D, k, \alpha)$. The x-intercept is defined by D (located at the two vertical red lines in this plot), while curvature is described by the shape parameter k .

Later, when discussing the set of model runs we perform, we refer to whether or not we are assuming “protection normalization,” which refers to whether we are using s or \hat{s} . When protection normalization is not assumed, the probability of a tract burning always goes down with increasing tract density, though the overall expected loss within the region may or may not go down depending on the value of the concavity parameter k . When protection normalization is assumed, the probability of any given tract burning will go up if other tracts in the region gain housing units.

While each aspect of the scaling function (D , k , α , and whether to normalize) represents an uncertainty, changes in these parameters may be thought of as manifestations of fire management policies. For example, currently there exists some (possibly regionally distinct) best values for each parameter. Whatever those may be, lowering the WUI/urban threshold D or decreasing expected losses within the vulnerable density range by decreasing the concavity parameter k would correspond to increased fire exclusion in areas below the current density. Such an exclusion might be achieved by suppression resources or vegetation management or fire

prevention activities. If it is the case that fire policy today is better described by the protection normalization feature, moving the the strict-reduction case could (perhaps) be achieved by increased fire suppression resources, since protection normalization is based on the assumption that those resources are simultaneously effective and constrained. However, as we will emphasize later, the discussion in this subsection is about likelihood of tracts falling in a fire perimeter, and not the losses that occur when a tract does fall within a perimeter—an equally important factor.

When performing our set of model runs, we run all our ICLUS cases using a low value of D (147 HH/km²) and a high value of D (1000 HH/km²) in an attempt to bound the possible range of this variable. For ICLUS, these bounds derive from the the bounds of the “suburban” density range used in ICLUS: Higher than 1000 HH/km² is deemed “urban,” while lower than 147 HH/km² is deemed “exurban.” The lower threshold that we use UPlan for falls halfway between the R1 and R5 residential classes in UPlan (one and five housing units per acre, respectively), and is therefore equivalent to 741 in HH/km² and second is 10 percent above R5 (equivalent to 1359 HH/km²). We consider this upper threshold to be somewhat unrealistically high (approximately 35 percent above our ICLUS high threshold), but chose it based on a desire to encompass most plausible outcomes, which would not be accomplished using the ICLUS thresholds due to the interaction of two particular features of the UPlan data: One is its coarsely spaced discrete density classes, and the other is that UPlan results show approximately 90 percent of new growth in all scenarios occurs at or above R5. Using all thresholds below R5 (which we explored) would convey artificially low sensitivity, while using thresholds above R5 will overestimate it somewhat, and since our emphasis is more on bounding, we chose to use the higher threshold. It is also worth noting that higher thresholds may be more appropriate when using smaller tracts. If density is evaluated at, say, the individual plot level, a single house may have extremely high density, but if amid other densely spaced houses, would certainly remain susceptible to being encompassed by wildfire.

3.3.3 Scenarios to Vary Exposure Within Grid Cells

Here we are interested in identifying $P(\tau_i \in \tau_{VEG})$, the probability that a given tract (and its associated housing) lies within a vegetated area. While $P_0(\tau_i \in \tau_F | \tau_i \in \tau_{VEG})$ and $s(V_i)$ describe probabilities contingent on how value (number of housing units) is distributed within a vegetated area, this element focuses on the distribution of tracts among vegetated areas. For our long-term scenarios, we know only the distribution of tract values within the region, R , along with the fractions taken up by various land uses. Therefore, to bound the changes in exposure, we would like to consider different scenarios for how housing values in the vulnerable density range are distributed over the vegetated area. This essentially involves specifying the joint distribution of V_i and vegetation status within the grid cell. In some sense, this may be considered equivalent to mapping the wildland-urban interface, though at an abstract level, since we do not consider actual geographic relationships within the grid cell. This is a simplification of the multifaced wildland-urban interface concept, which describes in general how development at the urban fringe transitions to wildlands, including the spatial relationships between vegetation and housing (Radeloff et al. 2005).

For near-term fire-planning efforts in small areas, this is actually a distribution that can be estimated by linking land cover data with geographic information on the location of housing structures. For our long-term scenario-based work, we do not attempt to actually estimate this relationship, but instead bound it by considering different cases for the prevalence of vulnerable tracts within the vegetated area of the region.

As discussed in Section 3.3, we assume that only vegetated tracts can support wildfires. Housing in the middle of an urban area or desert or amid cropland are not threatened by large wildfires of the sort modeled here. Vegetated tracts may still have housing structures on them, but not above a the WUI/urban density threshold D , otherwise the tract would be considered urban rather than vegetated. Therefore, we refer to tracts in this density range as “potentially exposed.” Potentially exposed tracts are deemed actually exposed (i.e., at risk for loss due to wildfire) if they are on vegetated land, while those located on bare land are excluded, as are tracts with densities above the WUI/urban density threshold .

In this modeling effort, we have a set of tract values V_i within each region, and we know the total number of vegetated tracts (N_{VEG}) within each region, in addition to total number of urban, nonvegetated, and water tracts. However, we do not know how the tract values map to vegetation status of each tract, which will significantly affect the expected value lost in a fire event. Therefore, to explore the range of possible expected losses that could arise depending on how value is distributed across vegetated and non-vegetated tracts, we consider three limiting distributions for the relationship between tract values and vegetated areas, which we frame in terms of the exposed value contained in the WUI. (Technically, these schemes allocate growth in all vegetated areas, but most exposed value lies within the WUI, so we use WUI as a shorthand and a conceptual focus when describing our exposure scenarios.)

- **High-exposure WUI.** Of potentially exposed tracts (i.e., those that are not so dense as to be considered urban), we assign those with the highest probability-adjusted values (that is, the highest values of $s(V_i) \times L(V_i)$ to the vegetated area). If there are more potentially exposed tracts than vegetated tracts, the first N_{VEG} highest value tracts among all potentially exposed tracts are assigned to the vegetated area, with the remainder assigned to bare or agricultural land and considered not at risk to wildfire loss. If there are fewer potentially exposed tracts than vegetated tracts, all potentially exposed tracts are assumed vulnerable. If we let τ_H be the set of the first N_{VEG} tracts with the highest probability-adjusted loss potential (i.e., $s(V_i) \times L(V_i)$), then in this scenario we can formally express our probability rules as follows:

$$P(\tau_i \in \tau_{VEG}) = \begin{cases} 1 & \text{if } \tau_i \in \tau_H \\ 0 & \text{otherwise} \end{cases} \quad (7)$$

- **Low-exposure WUI.** This is simply the reverse of the above: Of potentially exposed tracts, we assign the those with the highest probability-adjusted loss values to bare areas first. If there are sufficient bare tracts in a region to hold all potentially exposed tracts, then there is no risk of housing loss in this scenario and in that region R ; otherwise the

vegetated region is assigned the lower-valued tracts. If we let τ_L be the set of the first N_{VEG} tracts with the lowest probability-adjusted loss potential, then in this scenario we can formally express our probability rules as follows:

$$P(\tau_i \in \tau_{VEG}) = \begin{cases} 1 & \text{if } (\tau_i \in \tau_L) \\ 0 & \text{otherwise} \end{cases} \quad (8)$$

- **Neutral WUI.** In this case, we consider the chance of a tract falling within the vegetated area of R to be independent of the value in the tract. Specifically, it is “neutral” in the sense that there is no bias for development in or outside vegetated areas, but instead we assume that the likelihood of being within a vegetated area is simply equal to the fraction of open land taken up by vegetated area: N_{VEG}/N_{OPEN} , where N_{OPEN} is the number of non-urban and non-water areas. Therefore, every potentially exposed tract is considered vulnerable with a fractional expectation, rather than some tracts being completely safe and some being completely vulnerable. Formally:

$$P(\tau_i \in \tau_{VEG}) = \begin{cases} \frac{N_{VEG}}{N_{OPEN}} & \text{if } V_i/\alpha < D \\ 0 & \text{otherwise} \end{cases} \quad (9)$$

The first two schemes respectively maximize and minimize the value that will be lost in the event of a fire within the WUI, by adjusting what tract values are assumed to lie within vegetated areas. The third, neutral, scheme provides a middle case that assumes each tract and its value V_i has an equal chance of being within a vegetated area, and therefore an equal chance of being encompassed by a wildfire perimeter. Our model runs include each of these three WUI-exposure cases for every other parameter combination considered.

3.4 Loss Conditional on Tract in Fire Perimeter

The expected damages contingent on a tract falling within a fire perimeter are a function of the value on that land, decreased by some scalar that captures protection efforts at the micro-level: Factors such as defensible space, construction material, ratio of land value to improved value, and others—it is not necessarily the case that a structure falling within the perimeter of a large fire is destroyed. In our present model considering long-term scenarios, this scalar is assumed to be some constant parameter so that $L(V_i) = \lambda V_i$. In principle λ could be tract-specific and time-specific, but for this analysis we assume it is constant statewide, in which case it falls out in our relative risk calculations (described later). As noted earlier, for value units V we use number of housing units, though a more sophisticated future analysis may attempt predicting monetary housing values based on projections from the present day combined with regional characteristics. However, at present such detail is unlikely to contribute much useful information for a scenario exercise with the timescale we are considering. Additionally, λ does not act in some complicated fashion and instead merely scales expected losses directly, so the value gained by incorporating variations in λ into our scenarios is minimal.

3.5 Calculation of Aggregate Relative Risk

The output of our model lies at the end of a cascading chain of uncertainty, and we do not consider our results to be predictions, but rather view this work as exploring the implications of different plausible assumptions about how long-term fire risk is best described. However, we can still take steps to reduce error and increase the validity of our findings by careful consideration of our output measures. In particular, to the extent that our individual model results can be considered a statistical product, we can reduce variance of our results by considering aggregate relative risk at larger spatial scales, rather than placing great stock in the absolute outcomes within individual grid cells. Aggregating to larger geographic areas (specifically, the whole state) helps reduce the effects of variance among individual grid cells, because the impact of random error will be reduced relative to our outcomes of interest. To the extent that any systematic bias in our model scales with the magnitude of impacts, the ratio of future losses to present losses evaluated under common assumptions will be a more reliable outcome measure. Most of our results are therefore presented as aggregate statewide relative risk, using common assumptions except where explicitly stated. Specifically, for each combination of scenarios and model uncertainties, we assess the sum of grid cell-level expected losses according to the following formula:

$$RR_T = \frac{\sum_j E(LOSS)_{jT}}{\sum_j E(LOSS)_{j0}} \quad (10)$$

where RR is relative risk, j indexes over grid cells within the state, T references two future time periods (30 years centered around 2050 and around 2085), and $E(LOSS)$ is defined as in Equation 1. The base period in the denominator references losses simulated for 1961–1990 using climate simulated for 1961–1990 and estimated year 2000 population and vegetation fractions.

While aggregation can be useful, identifying the most appropriate spatial scale to use is actually not a trivial issue, because aggregation is not always better—in particular, it allows the most heavily weighted areas to mask what may be legitimate subregional effects. Therefore we consider maps that show grid cell spatial patterns, and we show statewide aggregates. We also added some summary statistics for UPlan performance aggregated for the Bay Area and Sierra foothills as an intermediate level.

3.6 Growth Patterns as Multi-faceted Driver of Fire Probabilities and Exposure

A unique contribution of our model is that fire probabilities and exposure are explicitly linked contingent on different development patterns throughout the state. Specifically, as mentioned in Section 3.2, population and the fraction of vegetated area within a given region is a significant predictor of wildfire probability. Of course, as development takes place across a landscape, the amount of vegetated area will change depending on the development pattern— as dense development occurs in previously vegetated areas, those areas will no longer be considered

vegetated or susceptible to wildfire. On the other hand, sparse development amid vegetated areas may not appreciably diminish the vegetated fraction of a region, but instead puts large amounts of housing at risk.

In our model, residential housing growth affects wildfire housing risk in multiple ways. First, new housing growth above the WUI/urban threshold density (D) is assumed to reduce the vegetated area if that growth occurs on a vegetated land. Therefore, under different growth scenarios of where high density growth occurs, vegetation may be more or less reduced. Second, as mentioned above, values above D are assumed not to be at risk for loss due to wildfire, which means that even without altering vegetated area, different values will be exposed to loss depending on different density distributions. Third, in protection normalization cases (Equation 6), the vegetated fraction factors into \hat{s} .

Thus the fire probabilities themselves are a function of the spatial distribution of new growth (and its density), and the value that may be lost depends on how densely it is distributed over the landscape. Figure 3 summarizes all the dependencies in the model, along with the data sources and algorithmic procedures. The algorithmic details of these linkages are described above, and in the appendices describing how we process the growth scenario inputs.

One aspect of Figure 3 that we have not paid much attention to is the vegetation allocation algorithm, which is also described in previous work (Westerling et al. 2011a; Bryant and Westerling 2009), with an edited version reproduced in Appendix A.2 here. The key feature of the algorithm is that, because we do not know where dense development (development above the WUI/urban threshold) will be placed within a grid cell relative to vegetation in the grid cell, we again consider three bounding scenarios:

- All new growth above the WUI/urban threshold (high-density growth) is placed in existing vegetated areas, thereby reducing the vegetation footprint (dubbed the “min” scenario because it minimizes vegetation)
- All new high-density growth is preferentially allocated to non-vegetated areas (the “max” scenario)
- All new high-density growth is assigned to vegetated area in accordance with what fraction of available land is vegetated (the “neutral” scenario)

These scenarios share conceptual similarity with the WUI exposure scenarios of Section 3.3.3, except that those focus on value below the WUI/urban density threshold, and these focus on the value above it.

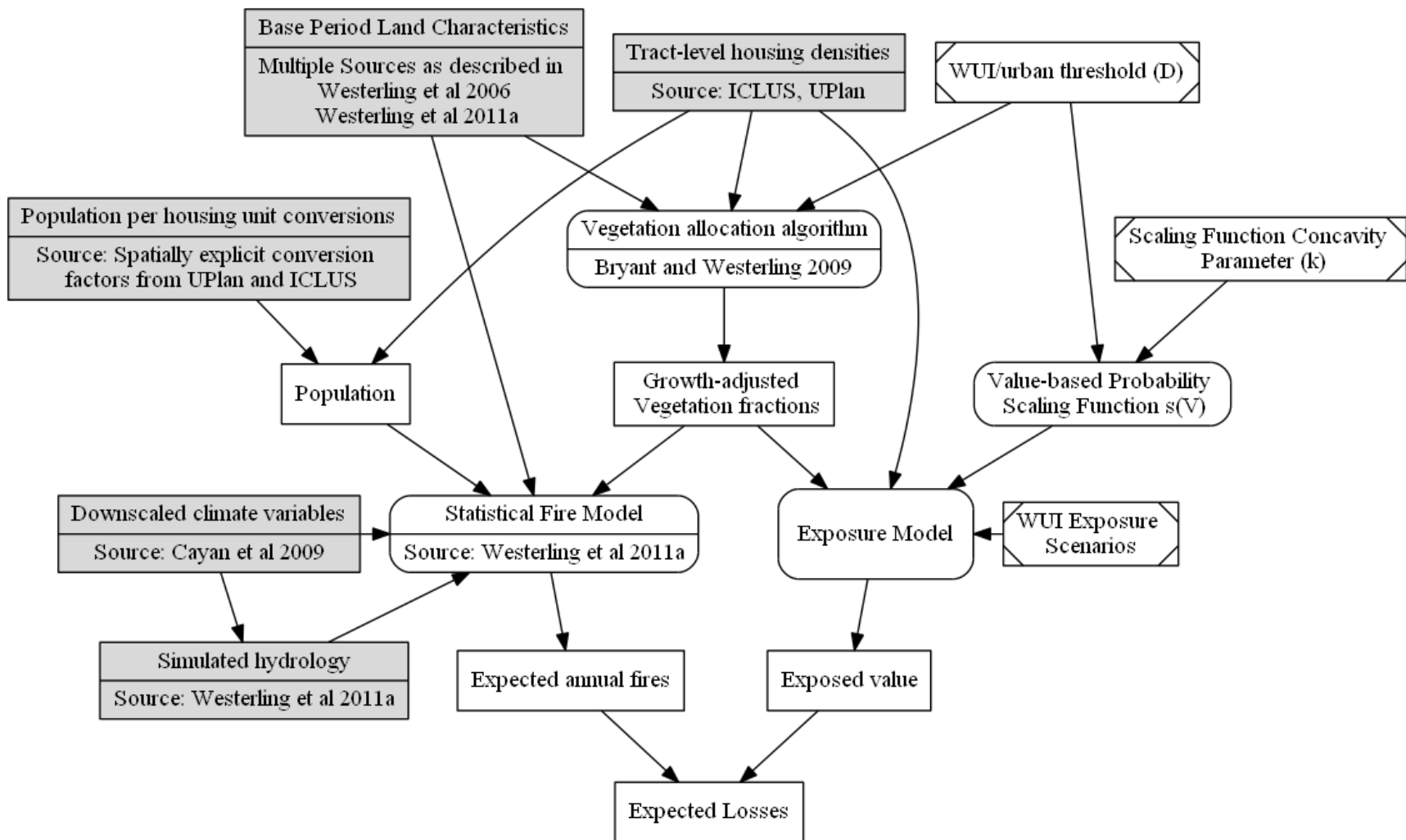


Figure 3: The implementation and detailed dependencies of the conceptual model in Figure 2. With the exception of initial UPlan and ICLUS data, all data sources and final outputs are at the level of the 1/8 degree grid cell, with the final product aggregated to the state level for most of our results. Grey boxes indicate external data products used as inputs, rounded boxes are functions or algorithms, rectangles are data products we produced, and rectangles with diagonal corners indicate parameters or scenario input we developed.

3.7 Integrating UPlan and ICLUS Data Sets for Scenario Runs

There are two related issues for the UPlan outputs that prohibit us from performing model runs that rely exclusively on UPlan data for our modeling inputs. The first, mentioned above, is that UPlan does not begin with or require a spatially explicit housing density map for the base year (2000). Rather, it utilizes a “pre-existing urban” layer that does not resolve residential density classes in developed areas, nor distinguish them from commercial and industrial land use. Rather, it assesses only whether each tract was deemed “urban” according to the criteria used by National Land Cover Database (NLCD: <http://www.mrlc.gov/nlcd2001.php>) or the California Augmented Multisource Landuse (CAML) map (<http://cain.ice.ucdavis.edu/caml>). The second issue is that all population in the base year is assumed to exist within this urban mask, which is problematic for wildfire risk analysis because both wildfire probabilities and wildfire-contingent damages are heavily influenced by the characteristics and population within the wildland-urban interface. This implies that without supplemental information, we cannot develop spatially explicit population estimates to drive the statistical model of wildfires. Furthermore, because our model assumes that housing within urban areas is not at risk for loss due to wildfire, relying only on the UPlan data would lead to zero risk for the base year. Essentially, UPlan’s assumptions are incompatible with our assumptions for modeling fire risk in the base year. To handle this, we use the ICLUS year 2000 data, with the value at risk in the base year lying only where ICLUS has densities below the WUI/urban threshold D , and not masked out by the UPlan pre-existing urban map.

Finally, there is one more challenge to using the UPlan data for fire risk assessment, which is that it utilizes different criteria for the base-year urban layer depending on county. The default is to use the CAML urban layer, but in counties where there is insufficient open space to allocate all new required growth for 2050, the pre-existing urban layer is reduced to the NLCD boundaries (classes 22–24 based on impervious surface cover), which has equal or smaller cover than CAML. This was done as a method of modeling in-growth or urban redevelopment in counties that were already highly urbanized. However, if used as-is within our fire loss modeling framework, it would introduce significant inconsistencies into our calculation of vegetation fractions when we compare future years to base years, because it would involve making assumptions about tract vulnerability that would vary in ways wholly unrelated to their actual vulnerability.

To address this situation, we calculate vegetation fractions for the baseline year and 2050 year in three different ways: One is using UPlan’s pre-existing urban layer, (a mix of NLCD and CAML as described above), and we also consider a full CAML and a full NLCD layer. In all cases we also count baseline ICLUS 2000 cells that are marked as commercial or lie above the WUI/urban threshold. We run these three layers for all our scenarios so we can assess the impact of the base-urban layer assumption and bound our estimates. We use a similar masking when identifying exposed values.

The detailed procedure for generating ICLUS and UPlan vegetation fractions is described at the algorithmic level in Appendix A.2.

3.8 Design of Computational Experiments

For our study design we produced two different full factorials of our emissions, climate, and growth scenarios crossed with various parameters designed to explore uncertainties in exposure: one for ICLUS and one for UPlan, as shown in Tables 2 and 3, respectively. In each table, the right two columns identify whether each factor has an influence on the probability of fires (P(F)), or the exposure, or both, reflecting the relationships shown in Figure 3.

Table 2: ICLUS Scenarios Factorial Study Design

Variable/Scenario	Levels	Affects P(F)	Affects Exposure
Emissions scenario	{B1, A2}	X	
Growth scenario	{low, mid, high}	X	X
Climate model	{NCAR PCM 1, CNRM CM 3.0, GFDL CM 2.1 }	X	
Vegetation allocation method	{min, neutral, max}	X	X
WUI exposure	{low, neutral, high}		X
WUI/urban threshold (D)	{147,1000} HH/km ²	X	X
Scaling function concavity parameter (k)	{.333, 1, 3}		X
Protection normalization	{no, yes}		X
Tract Spatial Scale*	{100, 200, 400, 800} (m)		X

*This refers to the level at which the density and spatial scale functions are evaluated—essentially the raster size to which the ICLUS data is aggregated. It applies to calculations of housing exposure to wildfire risk only—it does not affect calculations of vegetation fractions.

Table 3: UPlan Scenarios Factorial Study Design

Variable/Scenario	Levels	Affects	Affects
		P(F)	Exposure
Emissions scenario	{B1, A2}	X	
Growth scenario	{bau, smart, fire}	X	X
Climate model	{ NCAR PCM 1, CNRM CM 3.0, GFDL CM 2.1 }	X	
Vegetation allocation method	{min, neutral, max}	X	X
WUI exposure	{low, neutral, high}		X
WUI/urban threshold (D)	{741, 1359} HH/km ²	X	X
Scaling function concavity parameter (k)	{.333, 1, 3}		X
Protection normalization	{no, yes}		X
Base urban layer	{NLCD, UPlan, CAML}	X	X

For ICLUS, we only consider different tract spatial scales for the exposure side, not for the fire probability side, even though that ignores the potential for tract resolution effects on vegetation fraction. We conducted a sensitivity analysis which revealed that in this framework the risk of property loss was relatively insensitive to the effects of tract resolution on vegetation fraction, though the tract spatial scale does play a bigger role in determining exposure.

Finally, for results describing wildfire frequency and burned area, we also estimate scenarios where ICLUS populations and vegetation fractions are held constant at their year 2000 values, in order to see the effects of climate change and the various other parameters independent of population growth. Future work will include additional decomposition to assess driving factors.

Section 4: Results

As in Westerling et al. (2011a), wildfire burned area increases substantially statewide (Figure 4) under the A2 emissions scenarios by end of century. End-of-century B1 emissions scenarios and all mid-century scenarios have similar, lower-median increases. Note also that all of the A2 scenarios do pose higher tail risks, with greater spread above the median. Burned area in the UPlan and constant population scenarios do not differ appreciably in the statewide totals from the ICLUS scenarios. As in Westerling et al. (2011a, not shown), large increases in burned area are for the most part concentrated in forest areas in the Sierra Nevada, southern Cascades, and northern Coast Ranges, with lesser increases in mountain forest areas throughout the rest of the state.

4.1 Statewide Wildfire Area Burned under Varying Climate and Growth Scenarios

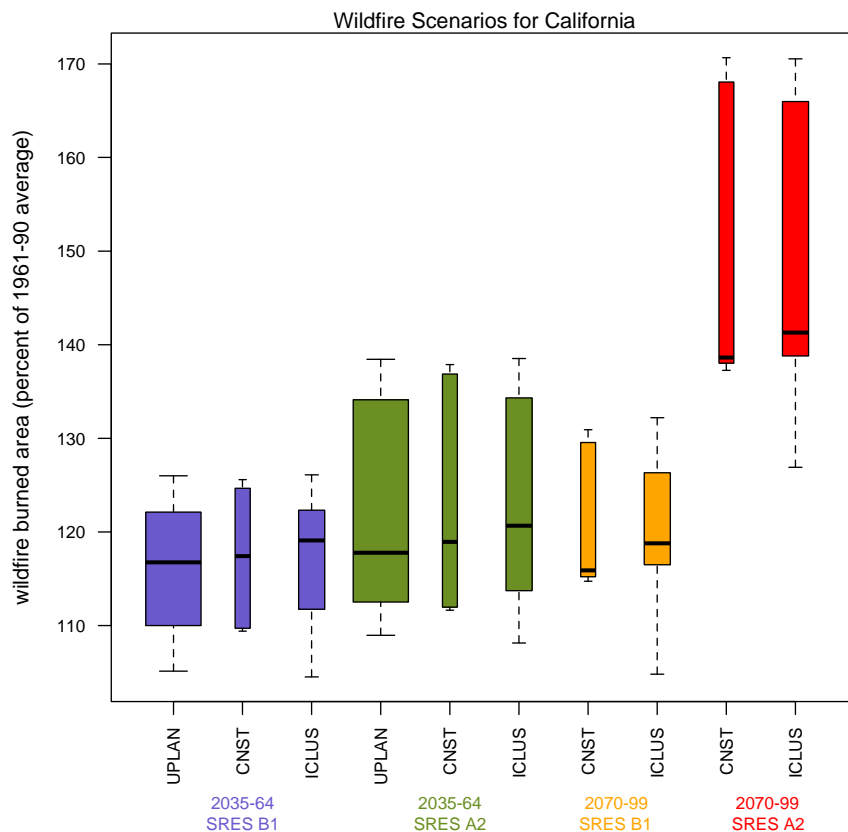
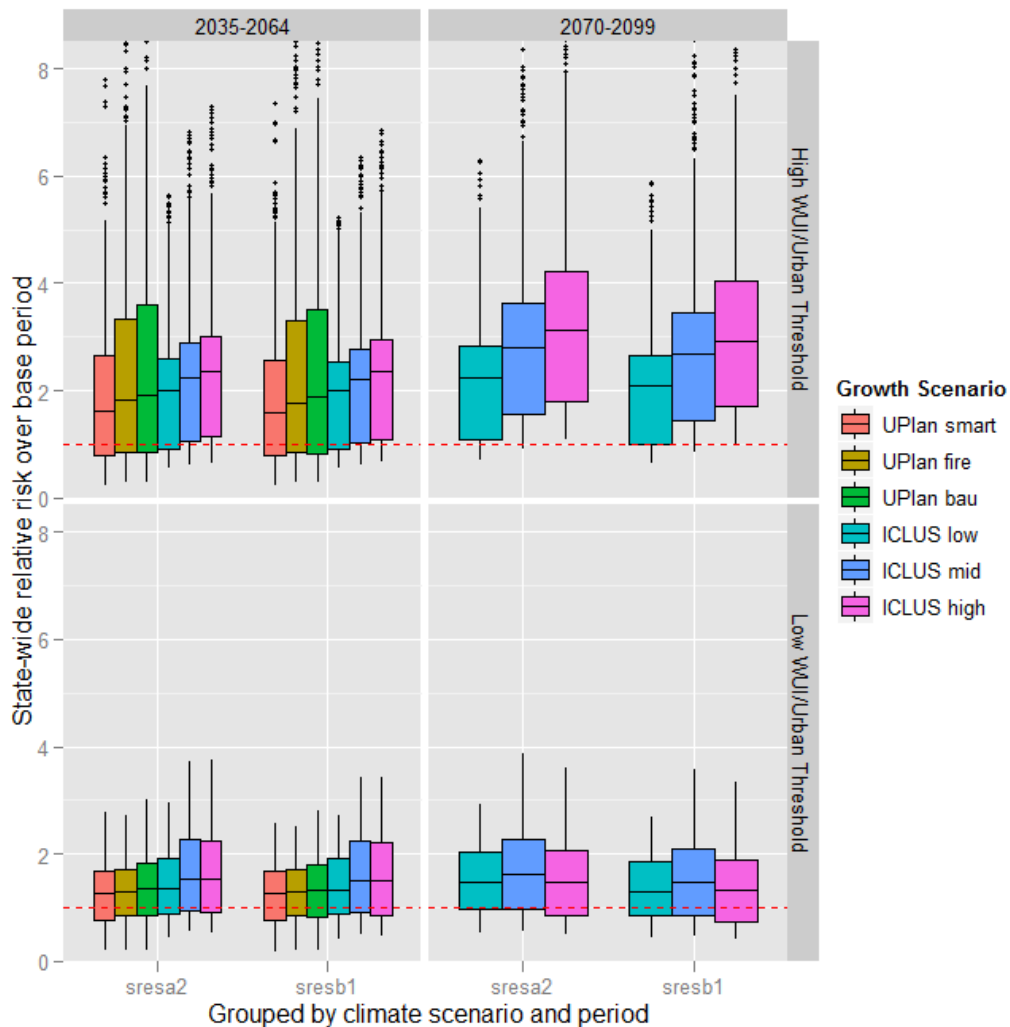


Figure 4: Statewide Wildfire Burned Area Scenarios for 2035–2064 and 2070–2099 Expressed as a Ratio to the Average Modeled for 1961–1990 (with Year 2000 Population and Land Use). Each UPlan boxplot summarizes 729 scenarios, while each ICLUS boxplot summarizes 162 scenarios. Constant (CNST) scenarios hold population and footprint constant at year 2000 levels; each CNST boxplot summarizes 54 scenarios.

4.2 Statewide Changes in Expected Losses under Varying Climate and Growth Scenarios



Notes: 28 ICLUS and 53 UPlan outliers between 8.5 and 12.09 are not shown; ICLUS and UPlan results capture different parameter assumptions. Vegetation fractions and WUI exposure held at “neutral” for the base year.

Figure 5: Statewide Relative Risk by Period, Broken Out by Growth Scenarios, Assumed WUI/Urban Thresholds, and Climate. Dashed red line represents no change in risk.

Figure 5 captures the range of results produced by the nearly 35,000 cases considered as part of our experimental design. Unlike Figure 4, which describes changes in area burned, Figure 5 shows the distributions of relative risk (RR as described in Equation 10) in each period of the twenty-first century, broken out by emissions and growth scenarios for two different housing density thresholds used to define the boundary between vegetated and urban (D). The variation associated with each individual box arises from different values for the remainder of our modeling parameters and other assumptions (e.g., scaling parameters, climate model used,

vegetation allocation scheme, and WUI exposure scenario). In this figure, each ICLUS box is capturing the variation of 648 individual parameter combinations and each UPlan box is capturing 486.

Even though there is wide variation within many emissions and growth combinations, the figure still identifies several clear trends. First, expected losses of housing units increase in future years under the vast majority of climate and growth scenarios and parameter uncertainty combinations. We can also see that the WUI/urban threshold (D) plays an important role in affecting both the magnitude and qualitative nature of the results. High threshold cases are associated with significantly higher relative risk in future periods, with medians between two and three in the 2070–2099 period, though ranging from below one to as high as ten. Low-threshold cases see almost all relative risks between one and two, with a small percentage negative. Qualitatively, high threshold cases follow the trend that scenarios with higher growth produce higher relative risk, while for the low threshold, the higher growth actually may reduce overall risk in some cases. This can be seen in the lower right panel, where the ICLUS high-growth case has a lower distribution than the ICLUS mid case. This can be explained by a combination of two factors: First, a lower threshold implies higher urban development, which implies smaller vegetated areas, which can reduce the probability of large fires. Second, lower thresholds exclude more value being considered exposed, via the action value-based scaling function $s(V_i)$.

4.3 Sources of Variation: Climate, Growth, and Land Use

Figure 5 also provides information about the relative importance of climate and growth scenarios in determining changes in residential wildfire risk, which we explore in more detail in this section. In particular, Figure 5 suggests that, at the state level, variation across growth scenarios is responsible for a greater variation in residential wildfire risk than changes across climate scenarios. This is indeed the case at the state level: A2 scenarios typically lead to greater wildfire risk over B1 scenarios in the 2070–2099 period, but the difference between them is small: 90 percent of cases lead to a relative increase in the range of -1 to 19 percent for A2 relative to B1. By contrast, the corresponding statistics when comparing ICLUS high growth to ICLUS low growth are: -24 percent and +72 percent. Note that these are statements about what the impact on risk could be when considering alternative futures, rather than parsing out responsibility for future increases in risk between climate and growth. Furthermore, because growth and fire management decisions are made on regional and smaller scales, it is also important to consider regional impacts, which do not necessarily represent statewide trends. We focus on these two aspects next.

4.3.1 Climate and Growth Impacts

Figure 6 and Figure 7 show spatial variation in relative residential wildfire risk for the San Francisco Bay and Sierra foothills under varying climate, growth, and model parameters;

comparing end-of-century climate and ICLUS growth scenarios to historical baselines.¹² In each case the values shown are ratios between expected losses for end-of-century scenarios and corresponding historical baseline scenarios. Growth and WUI exposure scenarios are held constant within each row, while climate scenarios are held constant in each column, with a B1 NCAR PCM1 climate scenario in the left column and an A2 GFDL CM2.1 climate scenario in the right column, and low growth in the first row and high growth in the second row. Thus, moving across columns shows the effect of climate holding everything else constant, while moving across the first two rows shows the effect of growth in the number of households. We can see that in the San Francisco Bay Area, the spatially explicit changes in wildfire risk mirror the larger statewide trends discussed above. The impact of climate is noticeable, but a more drastic change can be seen when moving from low growth to high growth. However, looking at the Sierra foothills, such trends are less clear. In fact, moving from A to B (low-growth/ low-climate change to low-growth/moderate-high-climate change) appears to increase risk in many places by as much or more than moving from A to C (low-growth/low-climate to a high-growth/low-climate). Though in both regions, their interaction in D produces the most dramatic changes.

¹² The change between low climate change and moderate-high climate change bounds the climate scenarios explored here. For a low climate scenario a run was used from the NCAR PCM1 model, which is less sensitive to forcing from greenhouse gases, forced with the lower SRES B1 emissions scenario. For the moderate-high climate change scenario, the GFDL CM2.1 model, which is more sensitive to greenhouse gases, was forced with the higher A2 emissions scenario. The term “moderate-high climate change” was used instead of “high climate change” because the warmest scenario explored here does not span the high range of potential scenarios available for California. This terminology is consistent with what has been used for the 2008 California Scenarios Project

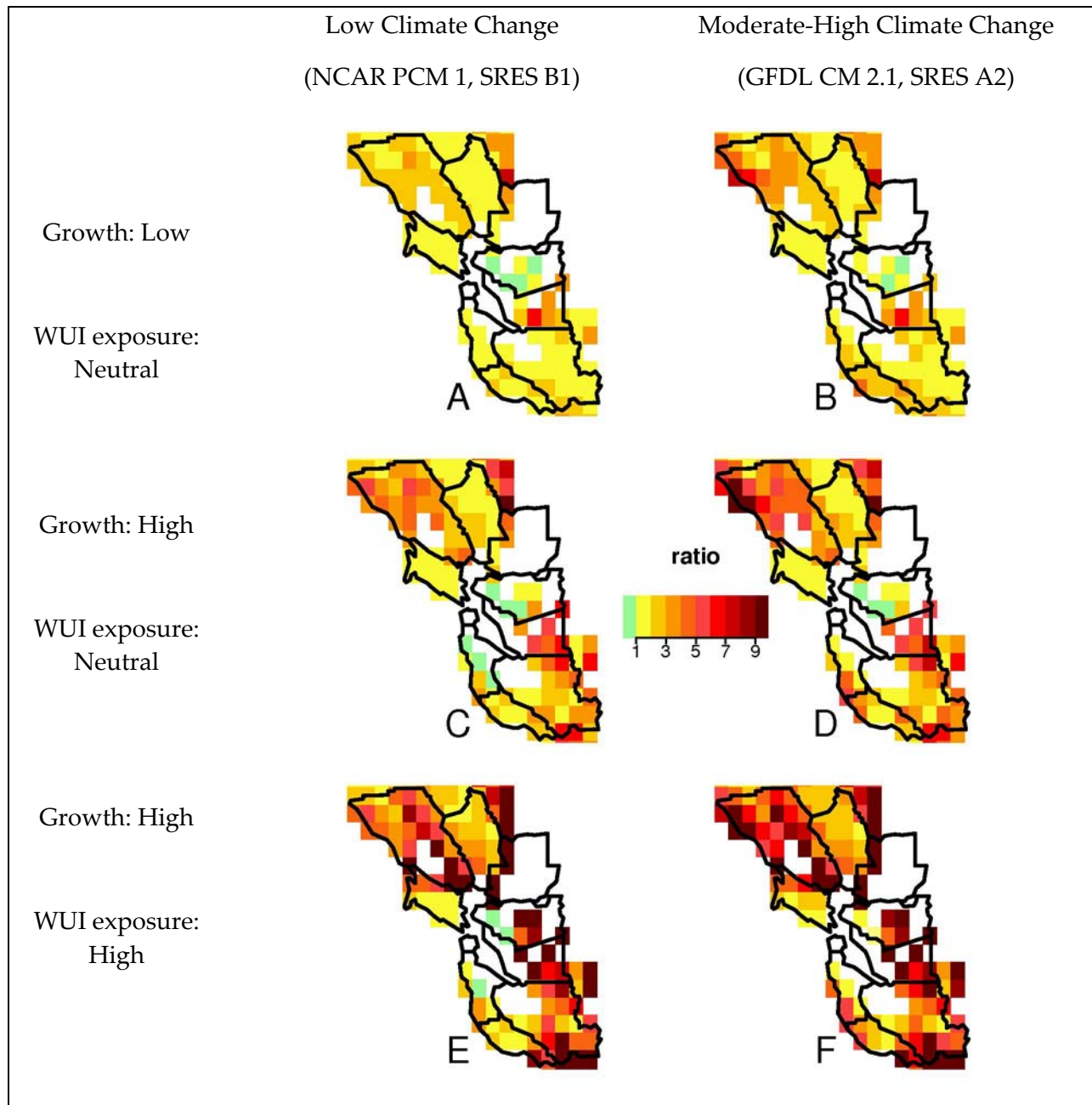


Figure 6: Spatial Variation in Wildfire Risk for the San Francisco Bay Area Using the Ratio of ICLUS 2070–2099 Scenarios to Risk Estimated for the Base Period. Six scenarios illustrate the effects of climate change, growth scenario, and WUI exposure on residential property risk. A relative risk of 1 is equal to no change; therefore, green cells represent reductions in risk. White cells are not modeled. Other parameters are fixed across all six scenarios: WUI/Urban threshold: 1000 HH/km², Vegetation allocation method (VEG): Neutral, Scaling function concavity parameter (k): 0.333, Protection normalization: yes, Resolution: 100 m.

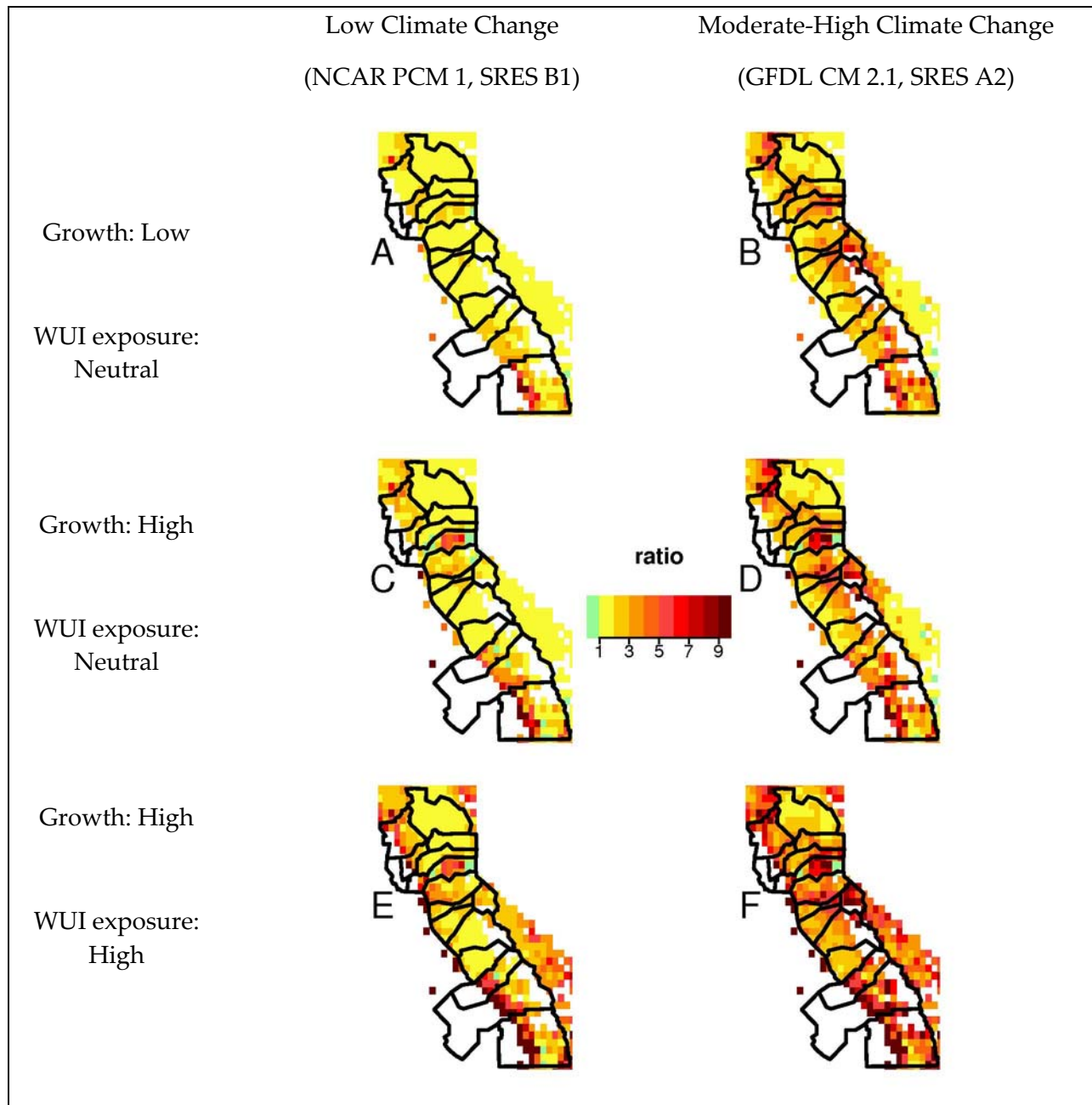


Figure 7: Spatial Variation in Wildfire Risk for the Sierra foothills Using the Ratio of ICLUS 2070–2099 Growth Scenarios to Risk Estimated for the Base Period: Six scenarios illustrate the effects of climate change, growth scenario, and WUI exposure on residential property risk. A relative risk of 1 is equal to no change; therefore, green cells represent reductions in risk. White cells are not modeled. Other parameters are fixed across all six scenarios: WUI/Urban threshold: 1000 HH/km², Vegetation allocation method (VEG): Neutral, Scaling function concavity parameter (k): 0.333, Protection normalization: yes, Resolution: 100 m.

4.3.2 Impact of Land Use Decisions

The first two rows of Figure illuminate how the relative impact of climate and growth may vary in diverse parts of the state. However, by considering the differences between the second row and the third row, we can see the marginal impact of development decisions on wildfire risk still holding all other parameters constant. Panels E and F describe the same high-growth situation as panels C and D, but consider different WUI housing allocations within each grid cell, with E and F representing cases in which more development occurs at highly exposed density levels within the vegetated areas of the wildland-urban interface. One can see that such a development pattern exacerbates the effects of more extreme climate and growth scenarios. In the Bay Area, the effects of greater high-exposure WUI development are particularly large in eastern Alameda and Santa Clara counties. (See Appendix A.3 for a county map of California with relevant counties labeled.) In the foothills on the west side of the Sierra Nevada, these effects are greatest in southern Sierra foothill counties of Madera, Fresno, and Tulare. On the east side of the Sierra Nevada, effects of high-exposure WUI development are particularly notable in Alpine county and northern Mono county under the warmer, drier SRES A2 GFDL CM2.1 scenario (B,D,F).

The UPlan scenarios for mid-century are able to more clearly illustrate the impact of different growth strategies, because population is held constant across the business-as-usual, smart growth, and fire threat avoidance scenarios. Therefore the only change is due to changes in growth patterns across the various UPlan development scenarios. The impact of the changes is summarized in Table 4, which shows how well each UPlan development scenario performed relative to the other scenarios, in the two regions mapped above. A few trends emerge: In general, “smart growth” outperforms “fire threat avoidance,” which in turn outperforms the “business-as-usual” case. Additionally, the relative impact of each scenario varies notably in both regions. In the San Francisco Bay area, the smart case can reduce expected losses by up to nearly 35 percent, while its strongest effect is less than half that in the Sierra foothills. We also see that, in the Sierra foothills, “smart growth” still shows the lowest expected losses, but that the “fire threat avoidance” scenario has many more positive scenarios relative to the San Francisco Bay area. For examples, it outperforms the “business-as-usual” scenario in only about one third of cases in the Bay Area, while it bests “business-as-usual” cases in 58 percent of scenarios in the Sierra foothills.

Table 4: Pairwise Performance of UPlan Scenarios for the San Francisco Bay Area and the Sierra Nevada Foothills

Bay Area	% cases with lower risk	Maximum reduction in risk (%)	Maximum increase in risk (%)	Sierra Foothills	% cases with lower risk	Maximum reduction in risk (%)	Maximum increase in risk (%)
smart relative to bau	99.6	34	0.5	smart relative to bau	100	15.7	NA
fire relative to bau	33.5	2.3	5.3	fire relative to bau	58.3	7.3	2.2
fire relative to smart	0.1	0.4	58.1	fire relative to smart	10.3	1.2	11.6

Table 4 supports two conclusions: Land use decisions matter, but the details of their implementation can (and do) vary across the state. Our model will generally show lower risk for scenarios that place more growth at higher densities, which the smart growth scenario does. However, because our model is highly sensitive to the threshold density, more robust conclusions would require an analysis using scenario data that features more finely resolved density classes, rather than the small number of discrete density classes used in the current UPlan scenarios.

In general, the residential wildfire risk scenarios are imposing a scaled household weighting on projected changes in wildfire. While all scenarios show the greatest increase in the expected area burned by large fires is projected to occur in mountain forests of northern California, the part of the Sierra Nevada that currently is given a high fire threat index by the California Department of Forestry and Fire protection is concentrated in the Sierra foothills, since much of the higher elevations are federal land. This is the same area where we see greater increases in risk, both area burned and expected losses, but also a relatively greater effect of the UPlan fire threat avoidance scenarios. It is also unfortunate that the UPlan scenarios do not extend to end of century, since the much larger increases in fire under end of century SRES A2 scenarios would provide a better test of the utility of the fire threat avoidance UPlan scenario.

By contrast, in the wildland-urban interface around the periphery of the San Francisco Bay Area, projected changes in large fire occurrence and burned area are much more modest, while proximity to large population centers guarantees rapid growth in households under the various population growth scenarios. Consequently, the changes in exposure are likely to drive the risk increases, and the density effects of smart growth have a much more noticeable effect.

4.4 Impact of Fire Risk Parameters

From a policy and management perspective, it is important to understand which factors impact magnitudes in a qualitatively important way. In particular, it is the case that under some parameter combinations, higher-growth scenarios lead to a decrease in expected fire losses, while in others it leads to an increase. What explains the difference?

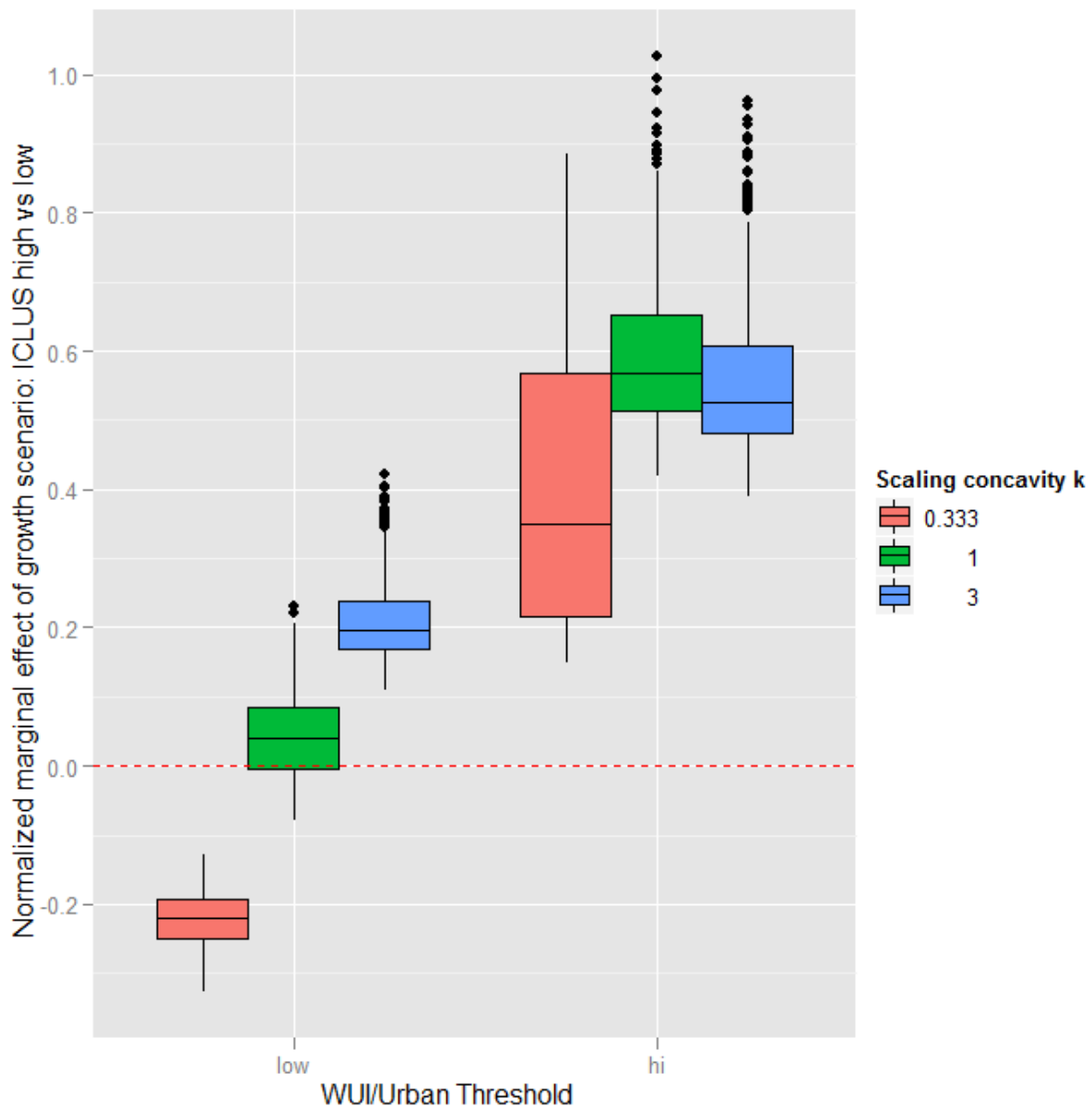


Figure 8: Relative Marginal Effect of High-Growth Compared to Low-Growth Scenario in 2070–2099, Grouped by Different Scaling Function Parameters. The interaction of the two has a strong influence on whether future growth increases or decreases expected losses statewide.

Figure 8 shows the impact of moving to a high-growth ICLUS scenario from a low-growth ICLUS scenario in 2070–2099, grouped by different combinations of the WUI/urban threshold (D) and the scaling concavity parameter k . In this figure, the y-axis represents the percentage change in 2070–2099 expected losses in a high-growth scenario relative to a low-growth scenario. For example, under the assumption that vulnerability to fire is best described by a low WUI/urban threshold and a small shape parameter ($k=1/3$), a high-growth scenario is likely to

lead to a 20 to 25 percent decrease in statewide expected losses relative to a low-growth scenario. By contrast, for a high threshold and large scaling parameter ($k = 3$), a high-growth scenario would lead to a 50–60 percent increase in expected losses.

Figure 8 clearly illustrates that those two parameters alone can determine the sign of the impact. If we think that fire behavior is accurately characterized by a low-threshold and a low-concavity parameter (the lower left), then we can expect a higher-growth scenario to lead to overall lower residential wildfire risk (i.e., paving over the risk), while high values for both implies that a high-growth scenario will lead to a large increase in fire risk. This suggests that, to the extent that the parameters describing exposure to wildfire are exogenous, it is important to learn about their true values in order to understand the impact that different growth scenarios are likely to have. Conversely, to the extent that these values can be affected by management, it provides an estimate of the importance of changing management schemes in ways that are reflected by lower thresholds and scaling parameters. Of course, policy levers in fire management and regional planning are far removed from simply adjusting the parameters of our scaling function. Rather, these are statistical-level descriptors of how the system may reflect different policies.

4.5 Discussion of Uncertainties and Caveats

While we go to great lengths to capture variation in outcomes due to different plausible modeling assumptions, there are nevertheless some that remain difficult to account for.

One issue we consider to be of concern is the construction of a fair base period at the grid cell level, due to compatibility of data sources. When we present relative risk compared to the year 2000 development crossed with 1961–1990 climate, our year 2000 data also rely on some modeling assumptions about land use, rather than drawing directly from a data set. In particular, our initial vegetation and urban fraction data rely on LDAS information, which was based on imagery collected in the early 1990s. For the maps presented here, we assume that growth happens according to the same rules between the time of LDAS data collection and the year 2000, as it does between LDAS and future years. But this need not be the case in reality. Growth may have proceeded under high-value WUI and high-vegetation-fraction conditions between LDAS and 2000, but could then plausibly shift to a low-value WUI case that also minimizes vegetation fractions in the future. In general, using consistent land use assumptions for the base year and future years represent entirely plausible scenarios, but also slightly reduces variation in the relative risk. To guard against false precision, our summaries of risk use the common baseline (“neutral” vegetation allocation and WUI exposure). We also emphasize that the ICLUS scenarios do not disaggregate population change and land use change. Future work may explore the disaggregation of these two factors.

Also, for UPlan, the use of a base year mask tends to reduce overall values exposed, and the criteria used to mask out those cells does not correlate perfectly with our WUI/urban threshold criteria that are applied to ICLUS base year data when used with UPlan, and that are applied to UPlan in future years. Another factor related to UPlan is that our WUI exposure scheme essentially overrides some of the UPlan modeling at the intra-grid-cell level, which is

particularly relevant for assessing the performance of the “fire-threat avoidance” scenario. To the extent that relocation of development only shifts UPlan growth patterns within grid cells, our results will not reflect that change—rather it is only where UPlan’s fire scenario shifts them to grid cells with lower risk as we evaluate it that the change is apparent.

In general, our model makes a variety of assumptions about certain factors remaining constant over space and time, which may impact interpretation of results on both those dimensions. One is that fire probabilities continue to respond to the presence of vegetation and population in the same manner as they have historically done. We also assume that the probability of a tract burning conditional on a fire occurring in the grid cell is independent of the vegetated area of that tract, and of the expected size of fires originating in the tract. Perhaps more significantly, we assume that expected losses contingent on a tract falling within a fire do not change over time or space—we devote more discussion to this issue and its relation to policy in the Conclusion.

Even where we do explore variation in parameters that lead to different levels of exposure, scenarios apply the same parameters across the state, and generally apply parameters consistently across time periods. It is theoretically possible that these parameters could vary in ways that exacerbate or mitigate the otherwise risk-increasing impact of new growth. For example, it may be that in areas with high and topographic relief, housing remains vulnerable at even higher densities than we have considered, or it may be that communities that are cognizant of their own high fire risk take greater steps to reduce their exposure. Such actions may vary across the state within time period, but may also change across time periods as well. Either of these could imply that the spatial patterns produced at the level of our 1/8-degree grid cell cells might not be robust.

Section 5: Conclusion

Residential property risk due to wildfire increases over the coming several decades under the vast majority of scenarios that we consider through the end of the century, although high growth can lead to reduced risk under a limited set of parameter combinations. Expected losses increase in almost all scenarios through mid-century, with low WUI/urban thresholds producing changes in risk that commonly range from a 20 percent decrease to a 100 percent increase; while a high urbanization threshold assumption shows many instances in which risk more than triples by mid-century. As a reference point for the magnitude of these changes, from 1990 to 2010, wildfires in state responsibility areas averaged about 130 million dollars of structure damage per year in California (California Department of Forestry and Fire Prevention 2011), which represents only a fraction of the total cost wildfires imposed on the state. It is also important to note that, even in the cases where we show a reduction in expected losses under high growth, that reduction is in part based on an assumption of fire protection response that increases with value—thus lowered expected losses may still be associated with significant increases in other wildfire-related costs.

Increases are due to a combination of climate, population growth, and changing exposure based on how development occurs, while the decreases are due to a combination of reduced vegetated area and reduced exposure due to growth at high densities. Overall, the relative impact of changes in exposure dominates when varying across scenarios considered here. While this is explained in large part by greater changes due to exposure alone, it is also a function of where growth occurs relative to changing climate and wildfire patterns.

Climate change is expected to increase the probability of large wildfires occurring in a substantial portion of the state, but the greatest increases are projected for forests in the mountains and foothills of northern California (Westerling et al. 2011a; see also National Research Council 2011; Spracklen et al. 2009; Westerling and Bryant 2008). This is largely because climate effects on fuel flammability tend to be important in these forests (Westerling et al. 2003; Littell et al. 2009). Warmer temperatures are associated with drier conditions and a longer fire season in western U.S. forests, as well as an increased incidence of large forest fires (Westerling et al. 2011b; Swetnam et al. 2009; Littell et al. 2009; Heyerdahl et al. 2008; Morgan et al. 2008; Westerling et al. 2006). In the statistical fire models used here, the probability of large fire occurrence tends to increase with temperature-related increases in summer drought, so the most extreme fire scenarios occur at the end of the century under the higher-emissions scenario examined here (SRES A2), and especially for the model with the greatest temperature sensitivity to the resulting greenhouse gas forcing (GFDL CM2.1) (see Westerling et al. 2011a).

ICLUS and UPlan growth scenarios tend to concentrate development in and around existing urban areas. These are typically in lower elevation areas with drier climates, where climate effects on fuel availability tend to be more important than on fuel flammability. Temperature is typically less important than antecedent precipitation as a driver of fire in these locations, and consequently the effects of climate change on fire risks are weaker and less certain than in the less-populated forest areas in northern California forests. As a result, the greatest increases in

households in terms of numbers and aggregate values potentially at risk in the state are in areas with weaker and less-certain changes in fire risks. Thus, the effects of growth scenarios tend to dominate those of climate scenarios at the statewide level.

Yet, statewide aggregates tend to obscure interesting details revealed by spatially explicit scenarios for wildfire and property risk. California's ecosystems and fire regimes are quite diverse, and as noted above the greatest increases in wildfire are projected for northern California forests, corresponding to end-of-century increases on the order of 100 to over 300 percent above the recent historical baseline (Westerling et al. 2011a; National Research Council 2011; Westerling and Bryant 2008). Much of this forest area is federal land reserved from residential use, under Park Service and Forest Service management. Growth in households is constrained to occur in private lands in the foothills and small mountain enclaves. In these areas of the state, our modeling indicates that residential property risks are highly sensitive to the growth in the number of households and their spatial footprint, relative to historical baselines. ICLUS scenarios indicate that, by end of century, rapid, sprawling growth in areas on the periphery of the Sierra Nevada could result in substantial increases in residential wildfire risks—with substantial areas projected to increase on the order of five to 10 times above the historical baseline—in a diverse array of communities from Tehama and Butte counties in the far north, to El Dorado, Amador, and Alpine counties in the north, to Madera, Fresno, and Tulare counties in the south (Figure 7F). And while patterns in the San Francisco Bay Area tended to more closely reflect parameter and scenario effects at the state level, it is visible from Figure 6 that risk increases vary significantly across the region depending on parameters and scenarios; for example, Panel 6E and 6F show drastic differences in risk along the coastal portion of Sonoma County, and these differences are explained mainly by the different assumptions about the interaction of new development with existing vegetation.

As we have seen, the range of potential outcomes for residential property losses for any given climate and growth scenario is large, suggesting a dominance of inherent uncertainty. Yet the dependency on key parameter values is clear and has implications for policy and research priorities. In particular, the results are largely driven by assumptions about our scaling function $s(V_i, D, k, \alpha)$, which describes how the probability of a tract falling within a fire perimeter varies with the value contained within the tract. This suggests the importance of data collection to characterize this scaling function more accurately, both in its shape and in how it may vary across the state. Doing so will be one step toward more confidently drawing growth and fire management implications using our modeling approach, which currently assumes several factors remain constant throughout the state and over time. At the same time, a very robust result of our scenario analysis is that “smart” growth strategies that concentrate growth in existing urban areas and at higher densities reduced expected losses by mid-century across the vast majority of scenarios.

While varying the parameters of our scaling function clearly revealed their driving role, we note that our analysis does not consider variation in one important parameter: λ , the expected loss contingent on property-specific protective efforts. This variable represents the fraction of value that is lost when a tract is encompassed by wildfire, and could be highly variable. To the extent

that new housing growth and residential landscaping follows best practices for fireproofing, and to the extent that future residents are able to successfully manage their property for greater resilience to fire, future expected losses will be proportionately lower. Indeed, recent state-level policy changes requiring increased defensible space (Public Resources Code 4291) and fire-resistant home construction (California Building Code Chapter 7A) should succeed in lowering this parameter over time in regions of severe fire hazard.

Lastly, from a public policy standpoint, it is also important to consider costs and benefits of growth and land management policy more broadly than just the fire risk context. Besides the important ecological impacts mentioned in the introduction, people build homes with low density in the wildland-urban interface because they perceive it to be a more desirable environment than other alternatives. It is also possible people may not take all fire-proofing steps available to them because they may deem them excessively costly or aesthetically undesirable. To the extent that homeowners may not be fully aware of and may not fully bear wildfire-related risks, there remains a role for government, land management agencies, and private sector actors such as property insurers to improve homeowner's understanding of the risk they bear when making such decisions, and to take actions to mitigate that risk.

References

- Allen, C. D., M. Savage, D. A. Falk, K. F. Suckling, T. W. Swetnam, et al. 2002. "Ecological Restoration of southwestern Ponderosa pine ecosystems: A broad perspective." *Ecological Applications* 12(5): 1418–1433.
- Bowman, D. M., J. K. Balch, P. Artaxo, W. J. Bond, J. M. Carlson, M. A. Cochrane, C. M. D'Antonio, R. S. Defries, J. C. Doyle, S. P. Harrison, F. H. Johnston, J. E. Keeley, M. A. Krawchuk, C. A. Kull, J. B. Marston, M.A. Moritz, I. C. Prentice, C. I. Roos, A. C. Scott, T. W. Swetnam, G. R. van der Werf, and S. J. Pyne. 2009. "Fire in the Earth System." *Science* 324(5926): 481–484, DOI: 10.1126/science.1163886.
- Bryant, B. P., and A. L. Westerling. 2009. Potential Effects of Climate Change on Residential Wildfire Risk in California. Public Interest Energy Research, California Energy Commission, Sacramento, California.
- California Board of Forestry. 1996. California Fire Plan. Archived 1996 version available at: http://cdfdata.fire.ca.gov/fire_er/fpp_planning_cafireplan.
- California Department of Forestry and Fire Protection. 2011. CAL FIRE Jurisdiction Fires, Acres, Dollar Damage, and Structures Destroyed. Fact sheet. http://www.fire.ca.gov/communications/downloads/fact_sheets/firestats.pdf. Accessed October 26, 2011.
- Cayan, D., M. Tyree, M. Dettinger, H. Hidalgo, T. Das, E. Maurer, P. Bromirski, N. Graham, and R. Flick. 2009. *Climate Change Scenarios and Sea Level Rise Estimates for the California 2009 Climate Change Scenarios Assessment*. California Climate Change Center, CEC-500-2009-014-F, 64 pages, August.
- Cohen, J. 2008. "The Wildland-Urban Interface Fire Problem." *Forest* 21.
- Dellasala, D. A., J. E. Williams, C. D. Williams, and J. F. Franklin 2004. "Beyond Smoke and Mirrors: A Synthesis of Fire Policy and Science." *Conservation Biology* 18: 976–986.
- Gesch, D. B., and K. S. Larson. 1996. Techniques for development of global 1-kilometer digital elevation models. In *Pecora Thirteen, Human Interactions with the Environment - Perspectives from Space*. Sioux Falls, South Dakota, August 20–22, 1996.
- Girardin, M. P., et al. 2009. "Heterogeneous response of circumboreal wildfire risk to climate change since the early 1900s." *Glob Change Biol* 15: 2751–2769, doi: 10.1111/j.1365-2486.2009.01869.x
- Gruell, G. E. 2001. *Fire in Sierra Nevada forests: A photographic interpretation of ecological change since 1849*. Missoula, MT: Mountain Press.
- Guyette, R. P., R. M. Muzika, and D. C. Dey. 2002. "Dynamics of an Anthropogenic Fire Regime." *Ecosystems* 5: 472–486.

- Hamlet, A. F., and D. P. Lettenmaier. 2005. "Production of temporally consistent gridded precipitation and temperature fields for the continental U.S." *J. of Hydrometeorology* 6(3): 330–336.
- Hansen, M. C., R. S. DeFries, J. R. G. Townshend, and R. Sohlberg. 2000. "Global land cover classification at 1 km spatial resolution using a classification tree approach." *International Journal of Remote Sensing* 21:1331–1364.
- Heyerdahl, E. K., P. Morgan, J. P. Riser, II. 2008. "Multi-season climate synchronized historical fires in dry forests (1650–1900), northern Rockies, U.S.A." *Ecology* 89: 705–716.
- Holmes, T. P., R. J. Hugget, and A. L. Westerling. 2008. "Statistical Analysis of Large Wildfires." Chapter 4 *Economics of Forest Disturbance: Wildfires, Storms, and Pests*, Series: Forestry Sciences, Vol 79. T. P. Holmes, J. P. Prestemon, and K. L. Abt, Eds., XIV, 422 p. Springer. ISBN: 978-1-4020-4369-7.
- Hurteau, M. D., A. L. Westerling, C. Wiedinmyer, B. P Bryant. In preparation. Projected California Wildfire Emissions for Climate Change and Development Scenarios through 2100.
- Intergovernmental Panel on Climate Change (IPCC). 2000. *Special Report on Emissions Scenarios: A Special Report of Working Group III of the Intergovernmental Panel on Climate Change* (Cambridge University Press: New York).
- Intergovernmental Panel on Climate Change (IPCC). 2007. *Climate Change 2007: The Physical Science Basis* (IPCC Secretariat, WMO, Geneva).
- Johnson, E. A. 1992. *Fire and vegetation dynamics*. Cambridge University Press: New York.
- Keeley, J. E., and C. J. Fotheringham. 2003. Impact of past, present, and future fire regimes on North American mediterranean shrublands. Pages 218–262 in T. T. Veblen, W. L. Baker, G. Montenegro, and T. W. Swetnam, editors. *Fire and climatic change in temperate ecosystems of the western Americas*. Springer-Verlag, New York.
- Kimball, J. S., S. W. Running, and R. Nemani. 1997. "An improved method for estimating surface humidity from daily minimum temperature." *Agric. For. Meteorol.* 85: 87–98.
- Krawchuk, M. A., M. A. Moritz, M-A. Parisien, J. Van Dorn, and K. Hayhoe. 2009. "Global Pyrogeography: The Current and Future Distribution of Wildfire." *PLoS ONE* 4(4): e5102. doi:10.1371/journal.pone.0005102.
- Krawchuk, M. A., and M. A. Moritz. 2011. "Constraints on global fire activity vary across a resource gradient." *Ecology* 92: 121–132.
- Lenihan, James M., Raymond Drapek, Dominique Bachelet, and Ronald P. Neilson. 2003. "Climate Change Effects on Vegetation Distribution, Carbon, and Fire in California." *Ecological Applications* 13:1667–1681. doi:10.1890/025295.

- Liang, X., D. P. Lettenmaier, E. F. Wood, and S. J. Burges. "A simple hydrologically based model of land surface water and energy fluxes for general circulation models." *J. Geophys. Res.* 99(D7): 14,415–14,428. July 1994.
- Littell, J. S., D. McKenzie, D. L. Peterson, and A. L. Westerling. 2009. "Climate and Ecoprovince Fire Area Burned in Western U.S. Ecoprovinces 1916–2003." *Ecological Applications* 19(4): 1003–1021.
- Maurer, E. P., A. W. Wood, J. C. Adam, D. P. Lettenmaier, and B. Nijssen. 2002. "A long-term hydrologically-based data set of land surface fluxes and states for the conterminous United States." *J. Climate* 15:3237–3251.
- Maurer et al. 2010. "The utility of daily large-scale climate data in the assessment of climate change impacts on daily streamflow in California." *Hydrol Earth Syst Sci* 14:1125–1138.
- Miller, J. D., H. D. Safford, M. Crimmins, and A. E. Thode. 2009. "Quantitative Evidence for Increasing Forest Fire Severity in the Sierra Nevada and Southern Cascade Mountains, California and Nevada, USA." *Ecosystems* 12: 16–32.
- Mitchell, K. E. et al. 2004. "The multi-institution North American Land Data Assimilation System (NLDAS): Utilizing multiple GCIP products and partners in a continental distributed hydrological modeling system." *J. Geophys. Res.* 109, D07S90, doi:10.1029/2003JD003823.
- Monteith, J. L. 1965. "Evaporation and the environment." *Symp. Soc. Expl. Biol.* 19: 205–234.
- Morgan, P., E. K. Heyerdahl, and C. E. Gibson. 2008. "Multi-season climate synchronized forest fires throughout the 20th century, northern Rockies, U.S.A." *Ecology* 89:717–728.
- National Research Council. 2011. *Climate Stabilization Targets: Emissions, Concentrations, and Impacts over Decades to Millennia*. The National Academies Press: Washington, D.C. 286pp.
- Penman, H. L. 1948. "Natural evaporation from open-water, bare soil, and grass." *Proceedings of the Royal Society of London* A193(1032): 120–146.
- Pierce, D. W., A. L. Westerling, and J. Oyler. In review. "Future Humidity Trends over the Western United States in Global Climate Models and the Variable Infiltration Capacity Hydrological Modeling System" *Journal of Climate*.
- Preisler, H. K., D. R. Brillinger, R. E. Burgan, and J. W. Benoit. 2004. "Probability based models for estimating wildfire risk." *International Journal of Wildland Fire* 13:133–142.
- Preisler, H. K., and A. L. Westerling. 2007. Statistical model for forecasting monthly large wildfire events in the Western United States. *J Appl Meteorol Climatol* 46:1020–1030.
- Preisler, H. K., A. L. Westerling, K. M. Gebert, F. Munoz-Arriola, and T. P. Holmes. 2011. "Spatially explicit forecasts of large wildland fire probability and suppression costs for California." *Int J Wildland Fire* 20:508–517.

- Radeloff, V. C., R. B. Hammer, S. I. Stewart, J. S. Fried, S. S. Holcomb, and J. F. McKeefry. 2005. The Wildland-Urban Interface in the United States. *Ecological Applications* 15:799–805.
- Spracklen, D. V., L. J. Mickley, J. A. Logan, R. C. Hudman, R. Yevich, M. D. Flannigan, A. L. Westerling. 2009. “Impacts of climate change from 2000 to 2050 on wildfire activity and carbonaceous aerosol concentrations in the western United States.” *Journal of Geophysical Research* 114, D20301.
- Stephens, S. L., R. E. Martin, and N. E. Clinton 2007. “Prehistoric fire area and emissions from California’s forests, woodlands, shrublands, and grasslands.” *Forest Ecology and Management* 251:205–216.
- Stocks, B. J., J. A. Mason, J. B. Todd, E. M. Bosch, B. M. Wotton, B. D. Amiro, M. D. Flannigan, K. G. Hirsch, K. A. Logan, D. L. Martell, and W. R. Skinner. 2002. “Large forest fires in Canada, 1959–1979.” *Journal of Geophysical Research* 108(D1, 8149): FFR 5-1–FFR 5-12.
- Strategic Issues Panel on Fire Suppression Costs. 2004. Large fire suppression costs—strategies for cost management. Available at (April 20, 2007): <http://www.fireplan.gov/resources/2004.html>.
- Strauss, D., L. Bednar, and R. Mees. 1989. “Do one percent of the forest fires cause ninety-nine percent of the damage?” *Forest Science* 35: 319–328.
- Swetnam, T. W., C. H. Baisan, A. C. Caprio, P. M. Brown, R. Touchan, R. S. Anderson, and D. J. Hallett. 2009. “Multi-Millennial Fire History of the Giant Forest, Sequoia National Park, California, USA.” *Fire Ecology* 5(3): 120–150, doi: 10.4996/fireecology.0503120.
- Syphard, A. D., V. C. Radeloff, J. E. Keeley, T. J. Hawbaker, M. K. Clayton, S. I. Stewart, and R. B. Hammer. 2007. “Human Influence on California Fire Regimes.” *Ecological Applications* 17:1388–1402. doi:10.1890/06-1128.1.
- Theobald, D. 2005. Landscape patterns of exurban growth in the USA from 1980 to 2020. *Ecology and Society* 10(1): 32.
- Thorne, J., J. Bjorkman, and N. Roth (University of California, Davis). 2012. Urban Growth in California: Projecting growth in California (2000–2050) under six alternative policy scenarios and assessing impacts to future dispersal corridors, fire threats, and climate-sensitive agriculture. California Energy Commission. Publication number: CEC-500-2012-009.
- Thornton, P. E., and S. W. Running. 1999. “An improved algorithm for estimating incident daily solar radiation from measurements of temperature, humidity, and precipitation.” *Agricultural and Forest Meteorology* 93:211–228.
- Verdin, K. L., and S. K. Greenlee. 1996. Development of continental scale digital elevation models and extraction of hydrographic features. In: *Proceedings, Third International Conference/Workshop on Integrating GIS and Environmental Modeling, Santa Fe, New Mexico*,

January 21–26, 1996. National Center for Geographic Information and Analysis, Santa Barbara, California.

- Westerling, A. L., T. J. Brown, A. Gershunov, D. R. Cayan, and M. D. Dettinger. 2003. "Climate and Wildfire in the Western United States." *Bulletin of the American Meteorological Society* 84(5) 595–604. DOI: 10.1175/BAMS-84-5-595.
- Westerling, A. L., H. G. Hidalgo, D. R. Cayan, and T. W. Swetnam. 2006. "Warming and Earlier Spring Increases Western U.S. Forest Wildfire Activity." *Science* 313: 940–943. DOI:10.1126/science.1128834.
- Westerling, A. L., and B. P. Bryant. 2008. "Climate Change and Wildfire in California." *Climatic Change* 87: s231–249. DOI:10.1007/s10584-007-9363-z.
- Westerling, A. L., B. P. Bryant, H. K. Preisler, T.P. Holmes, H. G. Hidalgo, T. Das, and S. R. Shrestha. 2009. "Climate Change, Growth and California Wildfire." *Public Interest Energy Research, California Energy Commission, Sacramento, California.*
- Westerling, A. L. 2010. "Wildfires." Chapter 8 in *Climate Change Science and Policy*, Schneider, Mastrandrea, Rosencranz, Kuntz-Duriseti Eds. Island Press.
- Westerling, A. L., B. P. Bryant, H. K. Preisler, T. P. Holmes, H. G. Hidalgo, T. Das, and S. R. Shrestha. 2011a. "Climate change and growth scenarios for California wildfire." *Climatic Change* In press. DOI 10.1007/s10584-011-0329-9.
- Westerling, A. L., M. G. Turner, E. A. H. Smithwick, W. H. Romme, and M. G. Ryan. 2011b. "Continued warming could transform Greater Yellowstone fire regimes by mid-21st century." *Proceedings of the National Academy of Sciences* 108(32):13165–13170.

Glossary

A	agricultural
AR4	IPCC Fourth Assessment
B	bare
CalFire	California Department of Forestry and Fire Protection
CAML	California Augmented Multisource Landuse
CNRM	Centre National de Recherches Météorologiques
D	density
FIPS	Federal Information Processing Standard
GCM	global climate model
GFDL	Geophysical Fluid Dynamics Laboratory
GPDs	generalized Pareto distributions
ha	hectares
ICLUS	Integrated Climate and Land Use Scenarios
IPCC	Intergovernmental Panel on Climate Change
km	kilometer
LDAS	Land Data Assimilation System
LRAs	local responsibility areas
m	meter
NCAR	National Center for Atmospheric Research
NCEP	National Centers for Environmental Prediction
NLCD	National Land Cover Database
NLDAS	North American Land Data Assimilation System
PIER	Public Interest Energy Research
RD&D	research, development, and demonstration
RR	relative risk
SERGoM	the Spatially Explicit Regional Growth Model
U	urban
V	Vegetation
VIC	Variable Infiltration Capacity
W	water
WUI	wildland-urban interface
N _{VEG}	number of vegetated tracts

Appendix A.1 Identifying New Populations for UPlan

UPlan data is provided on a 50 meter raster, with categorical encoding of housing and commercial densities. For calculating population, we assume that there are no residences on properties identified as light or heavy commercial, or industrial. Therefore, we create a new raster by substituting the per-acre household density into the raster according to the following mapping, provided in the UPlan description (Thorne et al. 2012).

Table A1: Raster Mappings for UPlan Housing Densities

Raster Value	Housing density (hh/acre)
9	20
10	5
12	1
13	.1
15	50
16	.5
17	0
18	0
19	0
20	10

Next, we make a similar substitution, replacing a raster encoding county level Federal Information Processing Standard (FIPS) codes with the county-specific population-per-household data used in the UPlan calculations. We then multiply those two rasters together to get per-acre population density by tract. Those values are then aggregated to the 1/8-degree grid cell and downscaled by the ratio of the tract area to an acre (2,500 square meters per tract to 4,046.85642 square meters per acre). Lastly, those are combined with the 1/8-degree estimates from ICLUS for the base year, which are calculated in a similar fashion. As discussed in the main text (Section 3.7), ICLUS data is used because the UPlan output does not include a year 2000 housing density map. The overall procedure is:

1. Combine UPlan 50 m rasters indicating household density with county-specific population-per-household data to develop a raster of population estimates at the 50 meter level.
2. Use point-in-polygon operations to sum populations within each grid cell. These provide the new populations only.
3. Combine the grid cell-level new populations for 2050 with the pre-existing grid cell level populations for 2000 from ICLUS.

Appendix A.2 Identifying Vegetated Areas Based on New Growth

This follows essentially the exact procedure as defined in the appendix to Westerling et al. (2009) and is included here for completeness. We first reproduce the salient points of that procedure, and then focus on the differences specific to UPlan.

In the limit of complete urbanization, it is clear that vegetation fraction is affected by encroaching human development, because a grid cell entirely covered by dense population would lack any sufficiently large vegetated space in which wildfires could exist. However, vegetation cover may be reduced by encroaching human development at intermediate scales as well, depending on how new growth is allocated. We model this allocation process as follows.

A given grid cell can be partitioned into the following disjoint areas, expressed as fractions of the grid cell they cover: Vegetation (V), urban (U), bare (B), agricultural (A), and water (W), with $V+U+B+A+W = 1$. These values exist for a baseline year, and when there is new urban growth with a footprint larger than the baseline urban fraction, it must be allocated to some combination of vegetation, bare, and agricultural land. To assess the range of impact that new growth may have on the vegetation fraction, we allot new growth in three different ways and consider the different impacts each method may have.

One is to maximize the wildfire-prone vegetation preserved, which is done by preferentially allotting new growth to the bare and agricultural areas before allotting any remaining growth to the vegetated areas:

$$VEG_{max} = V_0 - \max(0, N - (A+B))$$

Where N is the new urban footprint requiring allocation—that is, the difference between the urban footprint in a given time versus the urban footprint in the base year. In this formulation, if there is sufficient agricultural and bare land to accommodate all new growth, the vegetation fraction is not reduced at all.

Another option is to reduce the vegetation fraction by as much as possible, assigning all new growth to the existing vegetated area:

$$VEG_{min} = \max(0, V_0 - N)$$

These two allocation methods represent extreme bounds, and in reality, growth will tend to be distributed among all three land types. As a middle (“neutral”) option, we calculate the vegetation fraction assuming vegetated area is covered in direct proportion to how much area it occupies relative to agriculture and bare land:

$$VEG_{neutral} = \max(0, V_0 - N V_0 / (A + N + V_0))$$

To adapt these procedures for use with the UPlan scenarios, first we reclassify UPlan's new growth raster according to Table A1 as above, except that we assign commercial and industrial land use (categories 17, 18, and 19) to have effective density of infinity rather than zero, because here we care about land use, rather than population or value. A value of infinity will always be deemed to be above the WUI/urban threshold, and therefore always classified as unvegetated. We then convert mapped values to per-hectare values by multiplying the raw housing density value by the area ratio of hectares to acres (2.47), and then divide each tract value by four, to translate the per-hectare value into the 50 meter tract value. Each tract then holds a value that corresponds to the actual expected number of housing units on that tract (which may be fractional). We then apply the rules described in the main text for deciding whether each tract is classified as unvegetated or not. The overall procedure is described algorithmically below:

1. Align the 2000 ICLUS commercial and housing grids (100 m) grids with the UPlan 50 m data, and disaggregate the ICLUS grids to 50 meters.
2. For each tract, identify whether the tract is "too urban to burn" by assessing whether it meets at least one of the following criteria:
 - a. Was labeled commercial by ICLUS
 - b. Was labeled commercial or industrial by UPlan
 - c. Was labeled "pre-existing urban" by UPlan (with exceptions)
 - d. The combined housing density identified by UPlan and ICLUS is above the WUI/urban threshold.
3. Aggregate the fraction of all tracts labeled as "too urban to burn" by grid cell.
4. Identify what fraction is "new growth" relative to the urban fractions calculated using early 1990s LDAS data.
5. Diminish LDAS vegetation fractions according to three different scenario rules, one of which preserves as much vegetation as possible, one of which minimizes vegetation preserved, and one of which distributes new growth evenly among all cell types.

Appendix A.3: County Map for California



Figure A.3.1: County map for California with county names labeled for subregions discussed in Section 4